Robust Mathematical Symbol Recognition via Metric-Based Template Matching

B13201026 Yu-Hsiang, Chan,

B13201025 Kuan-Ting, Wu,

B13201008 Hui-Yu, Chou

December 22, 2025

Abstract

This study evaluates and compares the efficacy of three geometric distance metrics —L2 Pixel-wise Distance, Hausdorff Distance, and Chamfer Distance—in the recognition of fragmented and multi-component LaTeX symbols (e.g., $i, =, \div$). In contrast to deep-learning approaches, we propose a lightweight, deterministic framework that employs Connected Components Analysis (CCA) for adaptive grouping. The primary objective is to quantify and contrast how each metric performs in the presence of segmentation artifacts and structural noise. By benchmarking these metrics against a standard template database, this research identifies the optimal geometric approach for achieving high-precision shape similarity analysis in mathematical OCR.

1 Introduction

1.1 Problem Statement and Context

The conversion of static mathematical imagery into editable LaTeX code represents a significant challenge in document analysis due to the complex two-dimensional syntax and extensive character sets involved. While contemporary Math-OCR research is dominated by deep-learning models, these architectures often lack transparency and entail prohibitive

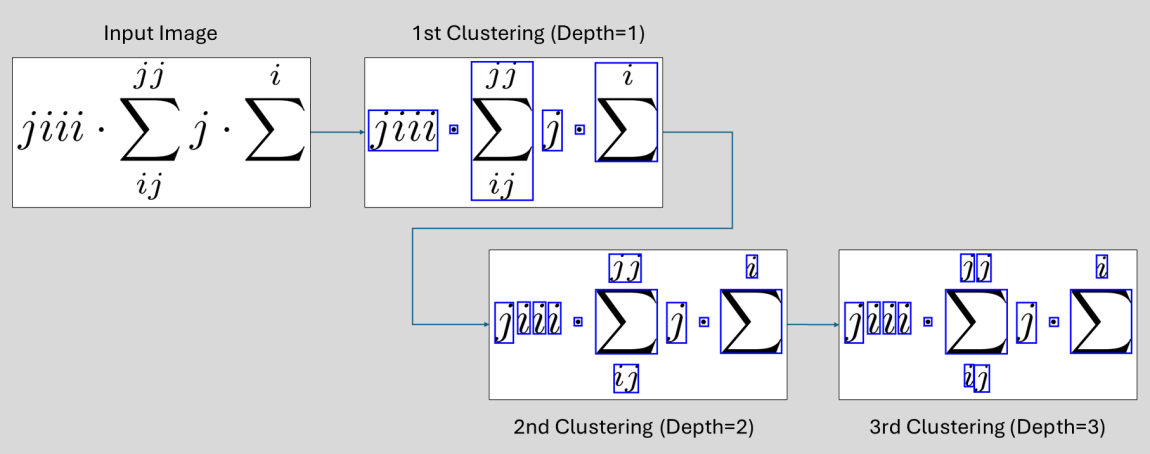

Figure 1: Example of the adaptive recursive clustering workflow.

computational overhead for simple printed expressions. This project explores a **rule-based approach** that leverages classical computer vision and geometric heuristics to provide a lightweight yet robust solution for symbol extraction and reconstruction.

A primary technical bottleneck in classical rule-based OCR is the **segmentation of disconnected components**. Mathematical notation is inherently prone to topological discontinuities, which can be categorized into two distinct classes:

- **Intrinsic Discontinuity:** Symbols naturally composed of isolated glyphs, such as $i, j, =, \div$, and $\approx$, where spatial proximity rather than physical connectivity defines the character.
- **Morphological Fragmentation:** Noise-induced breakage of continuous strokes. A representative case is the integral symbol ($\int$), where the thin, tapered terminals frequently detach from the primary body during binarization, resulting in isolated fragments.

Standard recognition pipelines relying on simple Connected Component Analysis (CCA) fail to synthesize these fragments into coherent semantic units because they lack a feedback mechanism to verify whether a cluster forms a valid symbol. To overcome this, we propose an **Adaptive Recursive Clustering** framework. As illustrated in Fig. 1, unlike static segmentation, our approach treats clustering as an iterative hypothesis-testing process: the system dynamically adjusts spatial weights and re-segments clusters based on the confidence of the matching result. This "recognition-driven segmentation" allows the system to intelligently re-group fragmented serifs or decompose over-clustered symbols.

Algorithm 1 Adaptive Recursive Clustering for Symbol Recognition

Input: Cluster C, Template library S, Similarity metric f_{sim}, Threshold τ

Output: Set of identified symbols R

function AdaptiveCluster($C, \text{depth}, r_x, r_y$)

$R \leftarrow \emptyset$

$(w_x, w_y) \leftarrow \text{UpdateWeights}(r_x, r_y)$ ▷ Determine weights from refinement ratios

$\mathcal{K} \leftarrow \text{GroupClusters}(C, w_x, w_y)$ ▷ Group new clusters by the new weights w_x, w_y

for each $k \in \mathcal{K}$ **do**

$(t^*, s^*) \leftarrow \text{FindBestMatch}(k, S, f_{\text{sim}})$ ▷ Match against templates

if $s^* < \tau$ **then**

$R_{\text{sub}} \leftarrow$ AdaptiveCluster($k, \text{depth} + 1, r'_x, r'_y$) ▷ Refine poorly matched cluster

$R \leftarrow R \cup R_{\text{sub}}$

else

$R \leftarrow R \cup \{(k, t^*, s^*)\}$

end if

end for

return R

end function

Main:

$R \leftarrow$ AdaptiveCluster($C, 0, r_x, r_y$)

return R

The success of this recursive loop is entirely dependent on the behavior of the similarity function f_{sim}, which serves as the primary heuristic for convergence. A similarity function that is overly sensitive to noise may trigger unnecessary sub-clustering, while an overly rigid similarity function may fail to recognize validly grouped but slightly deformed symbols. By substituting f_{sim} with different similarity functions, we not only identify which formulation performs best, but also analyze the respective advantages and disadvantages of each.

1.2 Background and Theoretical Framework

This research is grounded in **Metric Space Theory** and **Shape Analysis**. The core objective is to quantify the similarity between a candidate symbol cluster A and a template B within a normalized metric space $[0, 1]$, where 1 denotes an identical match. We represent symbols in two mathematical forms depending on the metric used:

1. As intensity functions $I(x, y) \in [0, 255]$ for pixel-wise comparison.
2. As finite sets of foreground pixel coordinates $P = \{p_1, p_2, \ldots, p_n\} \subset \mathbb{R}^2$ for geometric point-set matching.

To ensure scale invariance during comparison, the candidate cluster A is spatially rescaled to match the dimensions of template B before any distance computation.

1.2.1 L2 Pixel-wise Similarity

Unlike geometric point-set metrics, L2 similarity treats the symbol as a flattened intensity vector. This metric captures the global distribution of pixel intensities. Let $\mathbf{v}_A$ and $\mathbf{v}_B$ be the flattened intensity arrays of the rescaled images. The L2 distance is defined as:

$$D_{L2}(A, B) = \|\mathbf{v}_A - \mathbf{v}_B\|_2 = \sqrt{\sum_{i=1}^{N}(v_{A,i} - v_{B,i})^2} \tag{1}$$

To transform this into a similarity score $S_{L2} \in [0, 1]$, we normalize by the theoretical maximum distance $D_{max} = 255\sqrt{N}$, where N is the total number of pixels:

$$S_{L2}(A, B) = 1 - \frac{D_{L2}(A, B)}{255\sqrt{N}} \tag{2}$$

1.2.2 Hausdorff Similarity

The Hausdorff distance measures the degree of mismatch between two sets by identifying the "maximal outlier" distance. Let P_A and P_B be the sets of foreground coordinates. The directed Hausdorff distance from A to B is:

$$h(P_A, P_B) = \max_{a \in P_A}\left(\min_{b \in P_B}\|a - b\|_2\right) \tag{3}$$

The symmetric Hausdorff distance is $H(P_A, P_B) = \max\{h(P_A, P_B), h(P_B, P_A)\}$. To achieve normalization, we utilize the diagonal of the union's bounding box, Δ_{union}, as the scaling factor:

$$S_H(A, B) = 1 - \frac{H(P_A, P_B)}{\Delta_{union}} \tag{4}$$

1.2.3 Chamfer Similarity

The Chamfer distance provides a smoother measure of shape discrepancy by averaging the nearest-neighbor distances over all points. The symmetric Chamfer distance is defined as:

$$D_{CH}(P_A, P_B) = \frac{1}{|P_A|} \sum_{a \in P_A} \min_{b \in P_B} \|a - b\|_2 + \frac{1}{|P_B|} \sum_{b \in P_B} \min_{a \in P_A} \|b - a\|_2 \tag{5}$$

Because D_{CH} represents a sum of two mean distances, its upper bound is approximately $2\Delta_{union}$. The normalized similarity is:

$$S_{CH}(A, B) = 1 - \min\left(1, \frac{D_{CH}(P_A, P_B)}{2\Delta_{union}}\right) \tag{6}$$

1.3 Review of Existing Literature

The use of distance metrics for shape matching has a long history in computer vision. The **Hausdorff Distance** was significantly popularized for object matching by Dubuisson and Jain (1994), who introduced the Modified Hausdorff Distance (MHD) to increase robustness against outliers in edge-based matching[1]. Their work demonstrated that by utilizing an average of point distances rather than a strict maximum, the metric becomes far more reliable for character-like shapes.

Parallelly, **Chamfer Matching**, originally proposed by Barrow et al. (1977), has been a staple in shape-based recognition due to its computational efficiency when paired with distance transforms[2]. Borgefors (1988) further refined this into hierarchical structures, showing that Chamfer metrics are particularly effective for matching edge maps under slight deformations[3].

In the specific context of Mathematical OCR, early work by Kahan et al. (1987) identified that thin strokes and disjoint components are the primary causes of recognition failure[4]. While modern research has shifted toward deep-learning architectures (e.g., CNN-LSTMs), these models often function as "black boxes" and require massive

annotated datasets that are not always available for specialized or archaic mathematical fonts.[5]

1.4 Research Gap and Rationale

Despite the power of deep learning, there remains a significant gap in **lightweight, deterministic frameworks** that can handle fragmented mathematical symbols without heavy computational overhead. Most existing literature focuses on either high-level structural analysis (parsing the tree of a formula) or low-level character recognition, often bypassing the critical "mid-level" problem: *How to intelligently recompose fragmented components before they reach the classifier?*

There is a lack of comparative data on how classical geometric metrics (L2 vs. Hausdorff vs. Chamfer) perform specifically when embedded within an **adaptive, recursive clustering** loop. Specifically, the question of which metric best guides a rule-based system to "re-group" a detached integral serif or the dots of a $\div$ sign remains under-explored in the context of CPU-efficient, template-based OCR.

1.5 Research Objectives and Hypotheses

The primary objective of this study is to investigate the accuracy and the efficacy of three distinct geometric distance metrics within a lightweight LaTeX OCR framework governed by an **Adaptive Weighted Clustering** strategy. By prioritizing horizontal spatial coherence ($w_x > w_y$), this research seeks to determine which metric (or the metrics combination) most effectively guides the recursive synthesis of fragmented mathematical components.

Specifically, this research aims to:

1. Implement a deterministic algorithm that dynamically adjusts symbol segmentation boundaries based on real-time matching confidence scores.

2. Conduct a rigorous quantitative evaluation of **L2, Hausdorff, and Chamfer similarities**. The study will focus on their respective performance in terms of classification accuracy, tolerance to noise, and computational latency when processing complex mathematical symbols.

3. Specifically test the hypothesis that the **Chamfer Distance**, due to its L_1-like averaging property, provides superior robustness in recognizing morphologically fragmented symbols (such as detached integral terminals or multi-part operators) compared to the outlier-sensitive Hausdorff distance or the rigid L2 pixel-wise similarity.

2 Methods

2.1 Research Design and Computational Framework

This study employs an **experimental computational design** to evaluate the performance of the proposed adaptive OCR framework. The system is implemented in Python, chosen for its extensive library support and suitability for rapid prototyping of computer vision algorithms. The core architecture is designed to be modular, allowing for the seamless substitution of similarity metrics (f_{sim}) while maintaining a consistent recursive logic.

The software stack relies on the following specialized libraries:

- **NumPy & SciPy:** Utilized for high-dimensional matrix operations, distance transform computations, and spatial analysis (e.g., centroid calculation and KDTree-based nearest neighbor searches).
- **Pillow (PIL):** Employed for low-level image manipulation, binarization, and coordinate extraction.
- **XeLaTeX & PyMuPDF:** Used to generate and edit the LaTeX template library by rendering standard mathematical fonts into high-resolution bitmaps for ground-truth comparison.
- **Matplotlib:** Facilitates the visualization of clustering boundaries and the statistical analysis of recognition accuracy.

2.2 Hardware and Experimental Environment

To assess the ”lightweight” claim of our rule-based approach, experiments were conducted across two distinct hardware architectures representing different tiers of computational power:

1. **Desktop Environment (x86_64):** An Intel Core i5-10400 CPU, utilized for baseline performance benchmarking and extensive template matching.

2. **Mobile Environment (ARM):** A Samsung Exynos 1280 SoC, used to evaluate the feasibility of deploying the recursive algorithm on resource-constrained mobile devices.

2.3 Data Generation and Materials

The dataset consists of a **curated collection of printed mathematical expressions** derived from academic coursework and synthesized samples. To ensure a robust evaluation, the data includes both clean typeset expressions and samples artificially degraded to simulate **morphological fragmentation** (e.g., broken integrals and detached serifs). The template library (S in Algorithm 1) was generated using standard computer-modern fonts rendered at various scales to maintain scale-invariance during testing.

2.4 Experimental Procedure and Data Analysis

The study followed a multi-stage procedure:

1. **Algorithm Implementation:** Development of the recursive clustering logic and the integration of L2, Hausdorff, and Chamfer distance modules.

2. **Iterative Testing:** Running the recognition pipeline on the test set while varying the similarity threshold (τ) and the refinement ratios (r_x, r_y).

3. **Comparative Analysis:** Measuring two primary variables: **Recognition Accuracy** (percentage of correctly identified clusters) and **Computational Latency** (measured in milliseconds per symbol) across different devices and metrics.

2.5 Academic Integrity and Ethical Considerations

In accordance with academic standards, this research adheres to strict citation practices for all external libraries and theoretical frameworks utilized. No private or sensitive data was involved, as all mathematical samples were either self-generated or derived from public domain academic resources.

3 Results

3.1 Testcases Introduction

The proposed adaptive framework was evaluated using five distinct testcases, ranging from isolated characters to complex mathematical expressions. A library consisting of 459 symbols was utilized for template matching (See Appendix 5). The specific testcases are illustrated in Figure 2.

Case 01

$$t$$

Case 02

$$\int_{t_0}^{t} e^{-\alpha(t-s)} C(s)\,|x(s)|\,ds \leq \sup_{s\in[t_0,t]} |x(s)| \sum_{k=0}^{N} e^{-\alpha k} \int_{t-k-1}^{t-k} C(s)\,ds$$

Case 03

$$\int_{t_0}^{t} e^{-\alpha(t-s)} C(s)\,|x(s)|\,ds \leq \sup_{s\in[t_0,t]} |x(s)| \sum_{k=0}^{N} e^{-\alpha k} \int_{t-k-1}^{t-k} C(s)\,ds$$

Case 04

$$\int_{t_0}^{t} e^{-\alpha(t-s)} C(s)\,|x(s)|\,ds \leq \sup_{s\in[t_0,t]} |x(s)| \sum_{k=0}^{N} e^{-\alpha k} \int_{t-k-1}^{t-k} C(s)\,ds$$

Case 05

$$jiii \cdot \sum_{ij}^{jj} j \cdot \sum^{i}$$

Figure 2: Testcases 01–05: Ranging from basic characters (Case 01) to fragmented equations with Gaussian noise (Case 04) and complex index structures (Case 05).

Consistent with the research scope, Case 04 evaluates system behavior under stochastic noise without denoising. Because the primary objective focuses on **structural segmentation** and **geometric robustness**, Case 04 serves as a baseline for binarization limits and is excluded from the comparative analysis of metrics. (We still reproduce some results from Case 04 in the appendix 5)

The study conducted a rigorous evaluation of five metric configurations: L2 Pixelwise, Hausdorff, Chamfer, and two hybrid combinations (L2 + Hausdorff and L2 + Chamfer). The hybrid approach functions as a dual-gate verification: the system performs the second metric comparison only if the first (L2) meets the acceptance threshold; the result is

accepted only if both metrics independently satisfy.

3.2 Recognition Accuracy

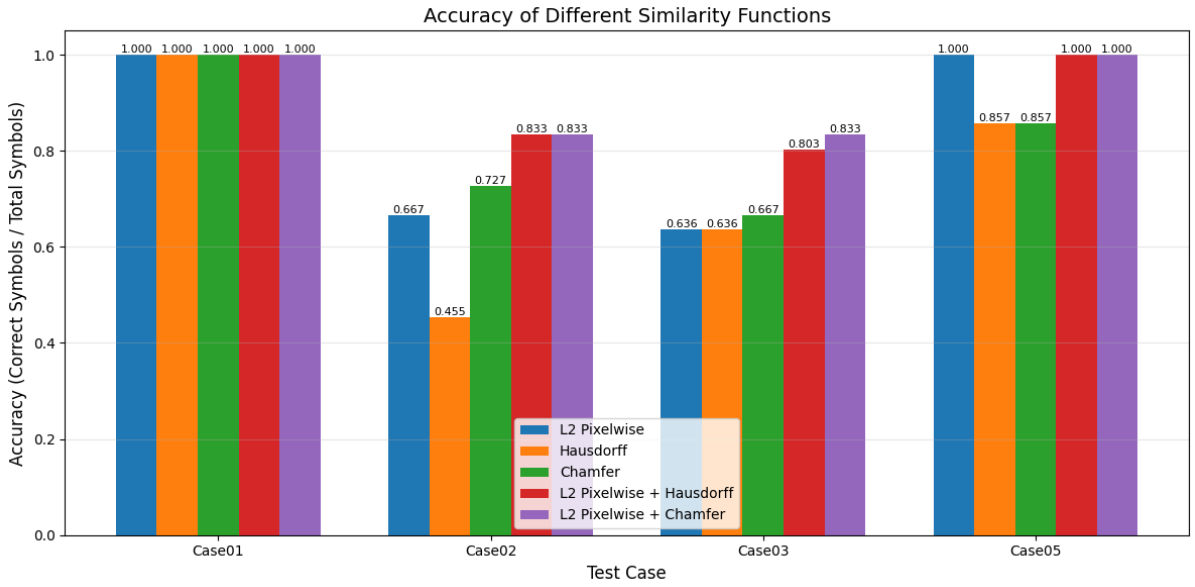

Figure 3: Accuracy of Different Similarity Functions across various testcases.

As illustrated in Figure 3, the accuracy findings highlight the following:

- **Hypothesis Testing (Chamfer Robustness):** In cases featuring morphological fragmentation (Case 02 and 03), the **Chamfer distance** achieved higher accuracy compared to the outlier-sensitive **Hausdorff distance**, which coincides with our prediction.
- **Hybrid Performance:** The **L2 + Chamfer** configuration achieved the highest overall accuracy across complex testcases, reaching in all cases.

3.3 Computational Latency and Efficiency

Computational latency was measured on an Intel i5-10400 PC environment (Figure 4 and Figure 5) and on a Samsung Exynos 1280 SoC smartphone (Figure 5).

The key findings from Figure 4 follow below:

- **Standalone Latency:** The simple Chamfer metric exhibited prohibitive latency, peaking at seconds for Case 03. Hausdorff distance similarly exceeded seconds in the same scenario.

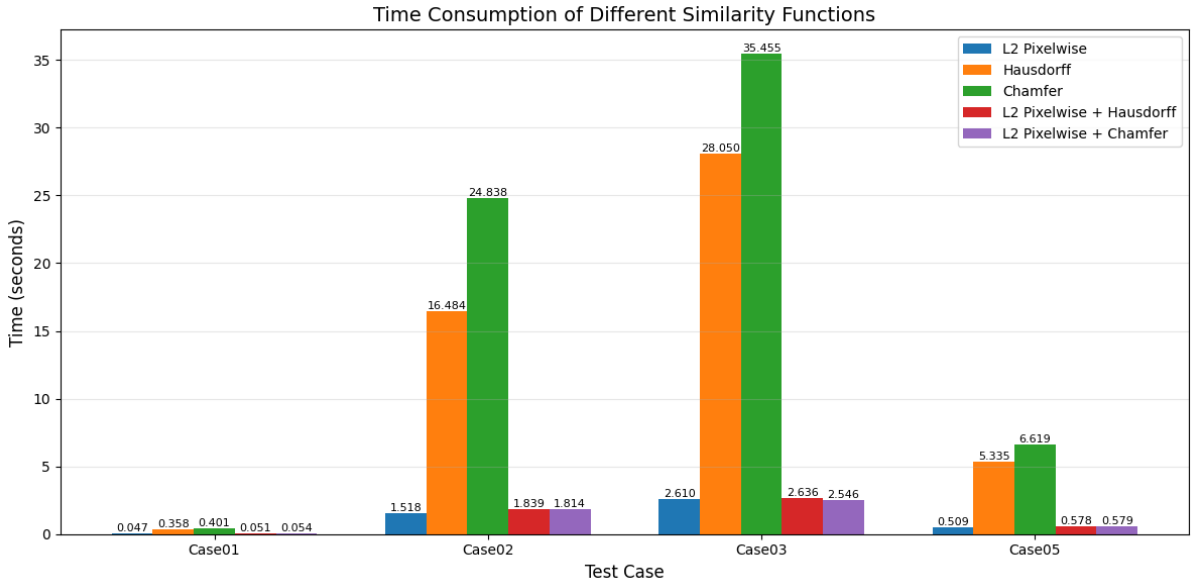

Figure 4: Time Consumption (seconds) of Different Similarity Functions. (tested on PC with Intel i5-10400)

- **Hybrid Optimization:** The **hybrid metric** (L2 + Hausdorff, L2 + Chamfer) not only significantly reduced latency to seconds, but also enhanced performance (Figure 3) in all cases. This indicates that the initial L2 gate effectively prunes the search space, avoiding redundant geometric computations for low-confidence matches.

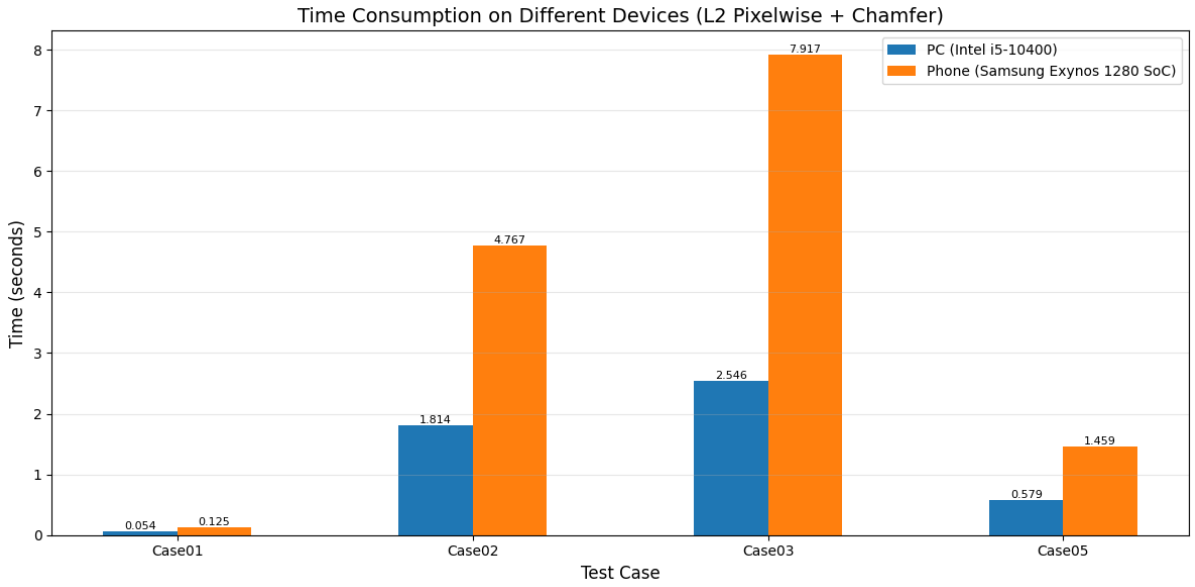

Figure 5: Time Consumption on Different Devices. (L2 Pixelwise + Chamfer)

The comparative results in Figure 5 show that for these normal cases, processing time remained below seconds on both devices, demonstrating the algorithm's efficiency even on ARM-based mobile processors.

4 Discussion

4.1 Interpretation of Results and Metric Performance

The experimental results demonstrate that the efficacy of the adaptive framework is highly dependent on the choice of similarity function. The **L2 similarity** serves as a moderate baseline; while it is capable of identifying general symbol shapes, it lacks the sensitivity required to distinguish between clusters with subtle geometric variations, such as the difference between $\int$ and $\int_t$. In contrast, **Hausdorff and Chamfer distances** exhibit a high degree of sensitivity to these "extra components," with the Chamfer metric being slightly more tolerant than Hausdorff, which aligns with our initial hypothesis regarding Chamfer' s averaging properties. However, this sensitivity proves to be a double-edged sword. Even within the adaptive clustering framework, standalone geometric metrics are prone to over-segmenting clusters due to their extreme sensitivity to minute or noise-induced components. This hyper-sensitivity can inadvertently trigger the recursive algorithm to further decompose a valid symbol, resulting in recognition accuracy that is lower than the more rigid L2 similarity in specific scenarios.

A significant breakthrough in this study is the success of the **Hybrid (L2 + Geometric) approach**. By utilizing L2 for initial pruning and reserving Hausdorff or Chamfer distances for secondary verification, the system achieves a "best-of-both-worlds" outcome. As seen in Figure 3 and Figure 4, the hybrid configurations maintain a computational profile nearly identical to the high-speed L2 metric while significantly exceeding its accuracy. This validates our proposed "dual-gate" logic as a viable method for real-time mathematical OCR.

4.2 Comparison to Existing Literature

Our findings are consistent with established computer vision literature. The superior performance of the Chamfer metric over the Hausdorff distance in fragmented cases (Case

02 and 03) reinforces the conclusions of **Dubuisson and Jain (1994)** regarding the necessity of averaging point distances to achieve robustness against outliers. Similarly, the efficiency of our framework supports the hierarchical structural advantages noted by **Borgefors (1988)** for shape matching under slight deformations.

Regarding the specific challenges of Mathematical OCR identified by **Kahan et al. (1987)**, our adaptive recursive clustering offers a deterministic solution to the problem of disjoint components and thin strokes. While modern research often favors deep-learning architectures such as CNN-LSTMs, our results demonstrate that a rule-based, lightweight approach can provide comparable accuracy for standard printed notation without the transparency issues or high data requirements of ”black box” models.

4.3 Limitations and Constraints

Despite the robustness of the hybrid framework, several limitations remain:

- **Image Quality Sensitivity:** The system's performance decreases significantly in over-exposed or low-contrast images. High exposure leads to ”fragmented” components that may require manual similarity threshold adjustments, while low contrast causes symbols to ”stick” together, causing the Connected Component Analysis (CCA) to fail at the initial stage.

- **Structural Complexity:** The current algorithm does not include logic for parsing complex mathematical structures such as square roots ($\sqrt{\dots}$) or fractions ($\frac{a}{b}$).

- **Orientation and Noise:** The implementation is sensitive to rotation and stochastic noise. As observed in Case 04, without specialized denoising or de-skewing pre-processing, recognition becomes unpredictable.

- **Template Scalability:** The template matching pipeline currently operates on a library of 459 symbols. This scale works well for mathematical expressions, but applying the same framework to domains with larger template collections would proportionally increase the search space, impacting runtime performance unless enhanced indexing schemes are introduced.

4.4 Broader Implications and Future Research

As a functional tool, this framework is sufficiently robust for daily digitization of standard printed mathematical resources, particularly on mobile devices where GPU-heavy deep-learning models are impractical. From a research perspective, this study provides a template for **explainable, deterministic OCR** that can be adapted for low-resource domains—such as archaic mathematical texts—where large annotated datasets for training neural networks do not exist.

Future work will focus on the following areas:

1. **2D Structural Parsing:** Developing a coordinate-based grammar to reconstruct recognized symbols into full, semantically correct LaTeX strings, including the proper nesting of fractions and radicals.

2. **Adaptive Pre-processing:** Integrating a self-tuning binarization and denoising layer to improve robustness against the exposure issues identified in our limitations.

3. **Hybrid Rule-Deep Learning Systems:** Investigating a model where the rule-based adaptive clustering handles the "mid-level" grouping of fragments, which are then passed to a lightweight CNN for final classification, potentially combining geometric logic with neural pattern recognition.

5 Conclusion

This study successfully developed and evaluated a lightweight, rule-based framework for LaTeX OCR based on an **Adaptive Recursive Clustering** strategy. By addressing the critical challenge of topological discontinuities in mathematical notation—specifically intrinsic and morphological fragmentation—we have demonstrated that deterministic algorithms remain a robust and efficient alternative to computationally intensive deep-learning models.

The key findings of this research highlight the following:

- **Metric Performance:** The **Chamfer distance** proved superior to the Hausdorff distance in recognizing fragmented symbols such as integral terminals ($\int$), confirming its robustness as a similarity metric due to its L_1-like averaging properties.

- **Hybrid Optimization:** The implementation of a **Hybrid (L2 + Chamfer) "dual-gate" logic** successfully balanced accuracy and speed. This configuration achieved the highest recognition accuracy in complex testcases while maintaining a computational latency nearly as low as the high-speed L2 Pixelwise baseline.
- **Computational Efficiency:** Benchmarks across distinct hardware architectures show that the proposed framework is capable of processing complex expressions in under 8 seconds on mobile ARM processors (Exynos 1280), validating its feasibility for real-time deployment on resource-constrained devices.

Beyond its functional utility as a digitization tool, this research contributes to the field of document analysis by providing an **explainable and deterministic methodology** for symbol reconstruction. Unlike "black-box" neural networks, our adaptive clustering loop offers transparency in how components are grouped and matched, making it particularly valuable for specialized scientific domains where large annotated datasets are unavailable.

In conclusion, this work bridges the gap between low-level component analysis and high-level character recognition. As digital transformation continues to demand efficient ways to process legacy printed scientific resources, the integration of geometric heuristics with adaptive recursive logic provides a foundation for the next generation of lightweight, accessible mathematical OCR systems.

References

[1] DUBUISSON M P JAIN A. A modified Hausdorff distance for object matching// Proceedings of 12th International Conference on Pattern Recognition: vol. 1. 1994: 566-568 vol.1. DOI: 10.1109/ICPR.1994.576361.

[2] BARROW H G, TENENBAUM J M, BOLLES R C, Parametric transformation system to match images to a geometric model//Proceedings of the 5th International Joint Conference on Artificial Intelligence (IJCAI). 1977: 659-663. https://www.ijcai.org/Proceedings/77-2/Papers/024.pdf.

[3] BORGEFORS G. Hierarchical chamfer matching: a parametric edge matching algorithm. IEEE Transactions on Pattern Analysis and Machine Intelligence, 1988, 10(6):

849-865. DOI: 10.1109/34.9107.

[4] KAHAN S, PAVLIDIS T, BAIRD H S. On the Recognition of Printed Characters of Any Font and Size. IEEE Transactions on Pattern Analysis and Machine Intelligence, 1987, PAMI-9(2): 274-288. DOI: 10.1109/TPAMI.1987.4767901.

[5] YUNTIAN DENG J L A M R, Anssi Kanervisto. Image-to-Markup Generation with Coarse-to-Fine Attention. Proceedings of the 34th International Conference on Machine Learning, 2017, 70: 980-989. https://proceedings.mlr.press/v70/deng17a/deng17a.pdf. DOI: 10.48550/arXiv.1609.04938.

[6] YU-HSIANG CHAN H Y C, Kuan-Ting Wu 114-1-ICM-project. [Online; accessed 22-Dec-2025]. 2025. https://github.com/D101028/114-1-ICM-project.

Appendices

Python Code for Key Methods

The following code demonstrates some essential functions used in our analysis. The full source code is available on Github[6].

Listing 1: L2 Pixelwise Similarity

```python
import numpy as np
from .cluster import ClusterGroup

def l2_similarity(base_cluster: ClusterGroup, cluster: ClusterGroup) -> float:
    """
    Compute the l2 distance of two images and normalize into [0, 1].
    """
    base_img = base_cluster.to_L()
    img = cluster.to_L().resize(base_img.size)

    # Compute L2 on flattened arrays
    arr1 = np.asarray(base_img, dtype=np.float32).ravel()
    arr2 = np.asarray(img, dtype=np.float32).ravel()

    l2_distance = np.linalg.norm(arr1 - arr2, ord=2)
    max_distance = np.sqrt(len(arr1)) * 255  # Maximum possible distance

    similarity = 1 - (l2_distance / max_distance)
    return float(np.clip(similarity, 0, 1)) # ensure the value is in [0, 1]
```

Listing 2: Hausdorff Similarity

```python
import numpy as np
from scipy.spatial.distance import cdist
from .cluster import ClusterGroup

def hausdorff_distance(A: np.ndarray, B: np.ndarray) -> float:
    """
    Computes the hausdorff distance between two sets of points A and B.
    """
    # A, B shape: (N, 2), (M, 2)
    if A.size == 0 or B.size == 0:
        return np.inf # 回傳最大值

    # 使用 cdist 計算成對距離矩陣 (N, M)
    dists = cdist(A, B, metric='euclidean')

    # Directed distances
    h_A_B = np.max(np.min(dists, axis=1))
    h_B_A = np.max(np.min(dists, axis=0))

    return max(h_A_B, h_B_A)

def hausdorff_similarity(base_cluster: ClusterGroup, cluster: ClusterGroup) -> float:
    """
    計算兩個 ClusterGroup 的 hausdorff 相似度。

    :param base_cluster: templates cluster
    :type base_cluster: ClusterGroup
    :param cluster: 欲比較之 cluster，先縮放到與 base_cluster 相同 size 再比較
    :type cluster: ClusterGroup
    :return: [0, 1] 區間的值
    :rtype: float
    """
    # resize
    h, w = base_cluster.get_bbox_hw()
    cluster = cluster.resize((w, h))

    arr1 = base_cluster.get_pixels_below_threshold()
    arr2 = cluster.get_pixels_below_threshold()

    if arr1.size == 0 or arr2.size == 0:
        return 0.0 # 若為空，返回 0 相似

    dist = hausdorff_distance(arr1, arr2)

    # 使用兩者聯集的對角線進行標準化 (最推薦，確保 ratio <= 1)
    all_pts = np.vstack([arr1, arr2])
    min_coords = all_pts.min(axis=0)
    max_coords = all_pts.max(axis=0)
```

```
    diff = max_coords - min_coords
    diagonal = np.sqrt(np.sum(diff**2))

    # 避免除以零
    if diagonal == 0:
        return 0.0 if dist == 0 else 1.0

    ratio = dist / diagonal
    return 1 - ratio
```

Listing 3: Chamfer Similarity

```
import numpy as np
from scipy.spatial import KDTree
from .cluster import ClusterGroup

def chamfer_distance(A, B):
    """
    Computes the chamfer distance between two sets of points A and B.
    """
    tree = KDTree(B)
    dist_A = tree.query(A)[0]
    tree = KDTree(A)
    dist_B = tree.query(B)[0]
    return np.mean(dist_A) + np.mean(dist_B)

def chamfer_similarity(base_cluster: ClusterGroup, cluster: ClusterGroup):
    # resize
    h, w = base_cluster.get_bbox_hw()
    cluster = cluster.resize((w, h))

    arr1 = base_cluster.get_pixels_below_threshold()
    arr2 = cluster.get_pixels_below_threshold()

    # 1. 處理空集合的情況 (避免 KDTree crash 或除以零)
    if arr1.size == 0 or arr2.size == 0:
        return 0.0 # 若一方為空，相似度為 0

    # 2. 計算 Chamfer Distance
    c_dist = chamfer_distance(arr1, arr2)

    # 3. 計算標準化基準 (對角線 D)
    # 建議使用兩者聯集的範圍，避免 ratio 變成負數 (因為 1 - ratio)
    all_pts = np.vstack([arr1, arr2])
    min_pt = all_pts.min(axis=0)
    max_pt = all_pts.max(axis=0)
    w_union = max_pt[1] - min_pt[1]
    h_union = max_pt[0] - min_pt[0]

```

```
    diagonal = (w_union**2 + h_union**2)**0.5

    if diagonal == 0:
        return 1.0 if c_dist == 0 else 0.0

    # 4. 標準化
    # 因為 chamfer_distance 回傳的是兩個 mean 的「和」
    # 所以最大值趨近於 2 * diagonal
    normalized_dist = c_dist / (2 * diagonal)

    # 限制在 [0, 1] 之間，防止浮點數運算誤差
    normalized_dist = min(1.0, normalized_dist)

    return 1 - normalized_dist
```

Data and Graphs

This section compiles the complete dataset and figures that are not included in the main article.

In the figures, red bounding boxes indicate clusters whose similarity scores do not meet the required threshold, while blue bounding boxes indicate those that do. Green dots denote the centroids of the corresponding clusters.

The data table includes the following columns:

Position (y, x, h, w) | Centroid (x, y) | Answer | Similarity | 2nd Similarity | Depth
These represent, respectively, the bounding-box coordinates of each recognized cluster, the centroid position, the closest matched answer, the similarity score, the second similarity score (set to 1.0 when unavailable), and the recursive depth at which the cluster was processed.

L2 Pixelwise Similarity

Similarity Threshold = 0.7

Figure 6: Case 01, L2

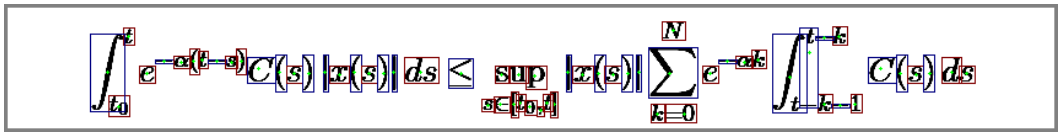

Figure 7: Case 02, L2

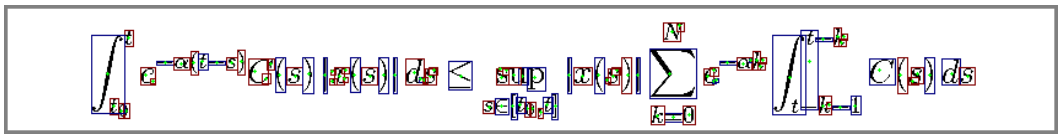

Figure 8: Case 03, L2

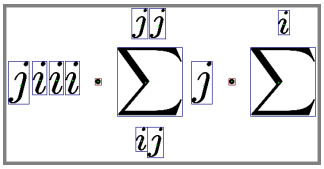

Figure 9: Case 05, L2

Case01-L2
Time: 0.04731249809265137s

Position (y, x, h, w)	Centroid (x, y)	Answer	Similarity	2nd Similarity	Depth
(12, 2, 12, 7)	(5, 18)	t	0.6501996994903936	1.0	0

Case02-L2
Time: 1.5179979801177979

Position (y, x, h, w)	Centroid (x, y)	Answer	Similarity	2nd Similarity	Depth
(22, 68, 61, 26)	(81, 52)	\int	0.8112695466053161	1.0	0
(72, 83, 15, 15)	(90, 80)	\text{k}	0.48111248463144873	1.0	0
(17, 95, 12, 7)	(98, 23)	t	0.6412090482077021	1.0	0
(48, 108, 12, 11)	(113, 53)	c	0.6302641111334014	1.0	0
(43, 121, 1, 13)	(127, 43)	-	0.8007422116349886	1.0	0
(40, 136, 8, 12)	(141, 44)	\alpha	0.5636751742760288	1.0	0
(34, 149, 19, 6)	(151, 43)	(	0.6800281140816784	1.0	1
(36, 156, 12, 6)	(158, 42)	t	0.5509637992098394	1.0	1
(43, 164, 1, 13)	(170, 43)	-	0.8007422116349886	1.0	0
(40, 178, 8, 8)	(182, 44)	\cdot	0.5336386048560049	1.0	0
(34, 187, 19, 6)	(190, 43)	)	0.6984232397013816	1.0	0
(41, 196, 19, 21)	(204, 49)	C	0.7489220313776552	1.0	0
(39, 219, 28, 7)	(221, 52)	(	0.7395491111297813	1.0	0
(48, 228, 12, 11)	(233, 53)	s	0.6442742711748131	1.0	0
(39, 241, 28, 7)	(245, 53)	)	0.7257545814123264	1.0	0
(39, 258, 28, 2)	(258, 52)	|	1.0	1.0	0
(48, 263, 12, 14)	(270, 54)	x	0.616991876571773	1.0	0
(39, 280, 28, 7)	(282, 52)	(	0.7395491111297813	1.0	0
(48, 289, 12, 11)	(294, 53)	s	0.6442742711748131	1.0	0
(39, 302, 28, 7)	(306, 53)	)	0.7208980172688736	1.0	0
(39, 314, 28, 2)	(314, 52)	|	0.972294003887706	1.0	0
(41, 324, 19, 26)	(336, 52)	L	0.5090748163863589	1.0	0
(42, 360, 22, 18)	(369, 53)	\leq	0.785439400295016	1.0	0
(75, 387, 8, 9)	(391, 79)	s	0.5725621765910893	1.0	0
(73, 397, 11, 11)	(401, 78)	\in	0.6917619024564499	1.0	3
(48, 398, 12, 10)	(402, 54)	\text{s}	0.6458485552135702	1.0	3
(69, 411, 19, 4)	(412, 78)	[	0.6489462442853158	1.0	5
(48, 409, 12, 14)	(416, 54)	\text{n}	0.627418862649586	1.0	4
(71, 415, 12, 6)	(417, 77)	t	0.5509637992098394	1.0	5
(76, 422, 10, 8)	(425, 80)	0	0.55120206820204	1.0	0
(48, 423, 17, 15)	(429, 55)	\text{p}	0.6809162258061873	1.0	0
(81, 432, 6, 4)	(434, 83)	,	0.5989129648050695	1.0	0
(71, 437, 12, 6)	(439, 77)	t	0.5509637992098394	1.0	0
(69, 443, 19, 4)	(445, 78)	]	0.6462592496082983	1.0	0
(39, 456, 28, 2)	(456, 52)	|	0.972294003887706	1.0	0
(48, 461, 12, 15)	(468, 54)	x	0.630689683546971	1.0	0
(39, 479, 28, 7)	(481, 53)	(	0.7126966312204062	1.0	0
(48, 487, 12, 12)	(493, 54)	s	0.6599998354065117	1.0	0
(39, 501, 28, 7)	(505, 53)	)	0.7120520177480982	1.0	0
(39, 513, 28, 2)	(514, 52)	|	1.0	1.0	0
(79, 525, 13, 10)	(529, 86)	k	0.5758825872966433	1.0	0
(33, 523, 39, 38)	(539, 53)	\sum	0.8047063556258368	1.0	4
(12, 534, 13, 17)	(542, 18)	N	0.6546182481105398	1.0	4
(79, 536, 13, 24)	(551, 86)	\longrightarrow	0.5455451124910109	1.0	0
(48, 567, 12, 11)	(572, 53)	c	0.6359622330989851	1.0	0

(43, 580, 1, 13)	(586, 43)	-	0.8007422116349886	1.0	0
(40, 594, 8, 12)	(600, 44)	\alpha	0.5101686826599887	1.0	0
(35, 607, 13, 10)	(611, 42)	k	0.5457637879691819	1.0	0
(22, 624, 62, 26)	(637, 56)	\int	0.7816781561936257	1.0	0
(17, 646, 63, 13)	(653, 36)	\therefore	0.7094034162632552	1.0	0
(24, 659, 1, 13)	(665, 24)	-	0.8007422116349886	1.0	3
(71, 661, 13, 10)	(665, 78)	k	0.5730413840756658	1.0	3
(16, 673, 13, 10)	(677, 23)	k	0.5457637879691819	1.0	3
(79, 672, 1, 13)	(678, 79)	-	0.8007422116349886	1.0	3
(71, 688, 13, 7)	(690, 78)	\text{l}	0.662755472202137	1.0	0
(41, 702, 19, 21)	(711, 49)	C	0.7515082146139705	1.0	0
(39, 725, 28, 7)	(727, 53)	(	0.7397297097623259	1.0	1
(48, 734, 12, 11)	(740, 54)	s	0.6045913594976304	1.0	1
(39, 747, 28, 7)	(751, 53)	)	0.7208980172688736	1.0	1
(41, 762, 19, 14)	(769, 52)	d	0.5913285615589079	1.0	1
(48, 776, 12, 11)	(781, 53)	s	0.6442742711748131	1.0	1

Case03-L2
Time: 2.610166311264038

Position (y, x, h, w)	Centroid (x, y)	Answer	Similarity	2nd Similarity	Depth
(22, 69, 61, 25)	(81, 52)	\int	0.8804873393286075	1.0	0
(73, 84, 11, 5)	(86, 78)	t	0.6441517116959318	1.0	0
(77, 91, 10, 3)	(92, 82)	(	0.6512793367097558	1.0	0
(77, 95, 10, 3)	(96, 82)	\}	0.5426730137681869	1.0	0
(18, 96, 11, 5)	(98, 23)	t	0.6471690877559237	1.0	0
(48, 109, 12, 10)	(112, 53)	e	0.6534720028715253	1.0	1
(57, 117, 2, 2)	(118, 58)	l	0.540958834049758	1.0	1
(43, 122, 1, 12)	(128, 43)	-	0.8007422116349886	1.0	0
(40, 136, 8, 11)	(141, 44)	\alpha	0.6401934020661277	1.0	0
(35, 150, 17, 4)	(151, 43)	(	0.6625122926824529	1.0	1
(37, 156, 11, 6)	(158, 42)	t	0.7364316773540476	1.0	1
(43, 164, 1, 12)	(170, 43)	-	0.8007422116349886	1.0	0
(40, 179, 8, 7)	(182, 43)	S	0.5909722944389066	1.0	0
(34, 188, 18, 4)	(190, 42)	)	0.6608101168813563	1.0	0
(41, 197, 19, 14)	(201, 50)	\mathcal{C}	0.6502051924982701	1.0	0
(53, 208, 6, 5)	(210, 56)	/	0.655018894273272	1.0	2
(41, 212, 7, 4)	(214, 44)	\bigstar	0.4852629735258074	1.0	2
(40, 219, 26, 6)	(221, 53)	(	0.7892597890311289	1.0	1
(48, 228, 12, 11)	(234, 54)	s	0.6855544392543803	1.0	0
(40, 241, 27, 7)	(245, 52)	)	0.7495430077581059	1.0	0
(40, 258, 27, 1)	(258, 53)	|	1.0	1.0	0
(50, 264, 2, 2)	(264, 50)	l	0.5325919575934173	1.0	3
(57, 263, 3, 4)	(264, 58)	\cdot	0.574616268382353	1.0	3
(48, 267, 12, 6)	(270, 54)	\text{l}	0.5866503869395692	1.0	0
(56, 274, 2, 2)	(274, 56)	l	0.5333415253571769	1.0	3
(48, 273, 3, 4)	(275, 49)	,	0.5552620223174003	1.0	3
(40, 280, 26, 6)	(282, 53)	(	0.7892597890311289	1.0	0
(48, 289, 12, 11)	(295, 54)	s	0.6855544392543803	1.0	0
(40, 303, 27, 6)	(306, 53)	)	0.761176477074688	1.0	0
(40, 315, 27, 1)	(315, 53)	|	1.0	1.0	0
(41, 325, 19, 13)	(331, 51)	d	0.6252310555453302	1.0	1
(56, 336, 2, 1)	(336, 56)	\blacksquare	0.9267089330849527	1.0	2
(56, 339, 3, 2)	(339, 57)	\blacksquare	0.6373230835302871	1.0	2
(49, 341, 11, 7)	(344, 54)	\text{S}	0.5349218701977737	1.0	2
(48, 344, 4, 5)	(347, 49)	\daleth	0.5445688167622816	1.0	2
(43, 360, 21, 17)	(369, 54)	\leq	0.7330452125125746	1.0	0
(75, 388, 8, 7)	(392, 79)	\mathcal{S}	0.5956813076357885	1.0	0
(48, 401, 1, 1)	(401, 48)	\blacksquare	0.6104547922684699	1.0	3
(49, 399, 11, 8)	(402, 55)	\text{S}	0.5588301773506583	1.0	3
(73, 398, 11, 9)	(402, 78)	\in	0.7280378688993686	1.0	0
(48, 404, 4, 3)	(406, 49)	]	0.5875483375106125	1.0	0
(69, 411, 19, 3)	(411, 78)	[	0.8584386780943228	1.0	4
(48, 409, 12, 8)	(412, 53)	\text{t}	0.622810586340846	1.0	4
(72, 415, 11, 6)	(417, 77)	t	0.7364316773540476	1.0	3
(48, 417, 12, 6)	(419, 54)	\text{l}	0.7602832897434025	1.0	3
(76, 422, 10, 3)	(423, 80)	(	0.5447595728141809	1.0	0
(76, 426, 10, 3)	(427, 80)	)	0.6522993797258271	1.0	3
(48, 424, 17, 13)	(429, 55)	\text{p}	0.7034994173092948	1.0	3
(81, 433, 6, 2)	(434, 83)	,	0.553059929809641	1.0	0
(72, 437, 11, 6)	(439, 77)	t	0.7364316773540476	1.0	0
(69, 444, 19, 3)	(446, 78)	]	0.8557352334757056	1.0	0
(40, 457, 27, 1)	(457, 53)	|	1.0	1.0	0
(48, 462, 12, 13)	(468, 54)	x	0.6789572519240435	1.0	0
(40, 479, 27, 6)	(481, 53)	(	0.7669114943388973	1.0	0
(56, 488, 3, 2)	(488, 57)	\blacksquare	0.6373230835302871	1.0	1
(49, 490, 11, 7)	(493, 54)	\text{S}	0.5349218701977737	1.0	1
(48, 493, 4, 5)	(496, 49)	\daleth	0.5445688167622816	1.0	1
(40, 501, 27, 6)	(505, 53)	)	0.6249594797343507	1.0	0
(40, 513, 27, 1)	(513, 53)	|	1.0	1.0	0
(79, 525, 13, 9)	(529, 86)	k	0.6414472515079733	1.0	0
(33, 524, 38, 36)	(539, 52)	\sum	0.8411653053740242	1.0	4
(12, 535, 13, 12)	(541, 18)	\lambda	0.6368609677265646	1.0	4
(85, 536, 5, 13)	(542, 87)	=	0.8319276568320804	1.0	0
(12, 546, 5, 4)	(547, 13)	\text{r}	0.6233790733514061	1.0	0
(79, 551, 13, 8)	(555, 85)	0	0.6662763727108042	1.0	0
(49, 568, 11, 6)	(570, 54)	\epsilon	0.6471086299745521	1.0	0
(48, 573, 5, 5)	(575, 49)	\rightharpoondown	0.6191103697605549	1.0	3
(58, 575, 1, 1)	(575, 58)	\blacksquare	0.927639548250941	1.0	3
(57, 577, 1, 1)	(577, 57)	\blacksquare	0.8887201389344801	1.0	3
(43, 581, 1, 12)	(586, 43)	-	0.8027651037744293	1.0	0
(40, 595, 8, 10)	(599, 44)	\alpha	0.557325814706936	1.0	0
(41, 605, 1, 1)	(605, 41)	\blacksquare	0.9267089330849527	1.0	0
(35, 608, 13, 4)	(610, 41)	l	0.5646925925594357	1.0	1
(44, 612, 4, 4)	(613, 46)	\lfloor	0.4984705874153188	1.0	2
(40, 614, 3, 3)	(615, 41)	\text{l}	0.5432348103038203	1.0	2
(22, 624, 62, 25)	(637, 55)	\int	0.7979709729152022	1.0	0
(18, 647, 62, 12)	(653, 42)	\therefore	0.7305096604442475	1.0	0
(24, 659, 1, 12)	(664, 24)	-	0.8007422116349886	1.0	3

(71, 662, 13, 8)	(664, 78)	k	0.6291418138851603	1.0	4
(76, 668, 3, 2)	(669, 77)	,	0.5239016535577095	1.0	4
(16, 674, 13, 4)	(676, 22)	l	0.5646925925594357	1.0	1
(79, 673, 1, 12)	(678, 79)	-	0.8027651037744293	1.0	0
(25, 678, 4, 4)	(679, 27)	\lfloor	0.4984705874153188	1.0	2
(21, 680, 3, 3)	(681, 22)	\text{l}	0.5432348103038203	1.0	2
(71, 688, 13, 6)	(690, 78)	1	0.7788550466860941	1.0	0
(41, 703, 19, 19)	(710, 49)	C	0.7785789898641748	1.0	0
(40, 726, 27, 6)	(727, 53)	(	0.614451802574221	1.0	0
(56, 735, 4, 6)	(737, 58)	\lfloor	0.5854212580690068	1.0	1
(48, 737, 11, 8)	(741, 52)	\text{s}	0.523505896315889	1.0	1
(40, 748, 27, 6)	(751, 53)	)	0.761176477074688	1.0	0
(41, 762, 19, 13)	(769, 52)	d	0.7235141696994037	1.0	1
(48, 776, 12, 11)	(782, 54)	s	0.6855544392543803	1.0	1

Case05-L2
Time: 0.5089051723480225

Position (y, x, h, w)	Centroid (x, y)	Answer	Similarity	2nd Similarity	Depth
(94, 4, 72, 34)	(24, 135)	j	0.8439512790537298	1.0	0
(94, 46, 56, 23)	(58, 126)	i	0.794103211752953	1.0	0
(94, 75, 56, 23)	(87, 126)	i	0.794103211752953	1.0	0
(94, 103, 56, 23)	(115, 126)	i	0.794103211752953	1.0	0
(124, 155, 9, 9)	(159, 128)	\cdot	0.675605899586397	1.0	0
(2, 219, 51, 26)	(234, 32)	j	0.8432893949510093	1.0	6
(208, 226, 40, 18)	(235, 231)	i	0.8264860018239998	1.0	6
(70, 194, 117, 111)	(242, 130)	\sum	0.9026867636132095	1.0	6
(208, 246, 51, 26)	(261, 238)	j	0.8432893949510093	1.0	6
(2, 250, 51, 26)	(265, 32)	j	0.8432893949510093	1.0	6
(94, 323, 72, 34)	(343, 135)	j	0.8439512790537298	1.0	1
(124, 388, 9, 9)	(392, 128)	\cdot	0.675605899586397	1.0	1
(70, 426, 117, 111)	(474, 130)	\sum	0.9026867636132095	1.0	4
(6, 474, 40, 18)	(483, 29)	i	0.8264860018239998	1.0	4

Hausdorff Similarity

Similarity Threshold = 0.9

Figure 10: Case 01, Hausdorff

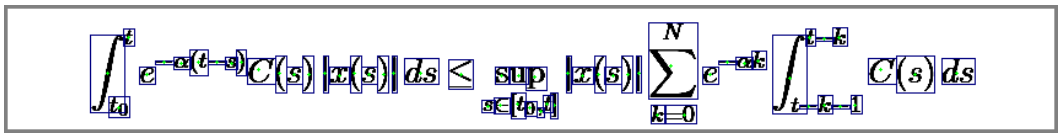

Figure 11: Case 02, Hausdorff

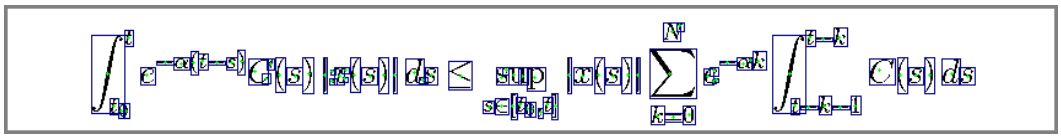

Figure 12: Case 03, Hausdorff

Case01-H
Time: 0.35808825492858887

Position (y, x, h, w)	Centroid (x, y)	Answer	Similarity	2nd Similarity	Depth
(12, 2, 12, 7)	(5, 18)	t	0.9301569704230421	1.0	0

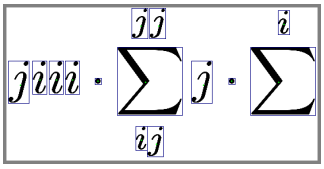

Figure 13: Case 05, Hausdorff

Case02-H
Time: 16.48368000984192

Position (y, x, h, w)	Centroid (x, y)	Answer	Similarity	2nd Similarity	Depth
(22, 68, 61, 26)	(81, 52)	\angle	0.9039458397395735	1.0	0
(72, 83, 15, 15)	(90, 80)	\Longleftarrow	0.9074730492069052	1.0	0
(17, 95, 12, 7)	(98, 23)	t	0.9301569704230421	1.0	0
(48, 108, 12, 11)	(113, 53)	e	0.9415793762163014	1.0	0
(43, 121, 1, 13)	(127, 43)	-	0.9600319616511285	1.0	0
(40, 136, 8, 12)	(141, 44)	|	0.926829268292683	1.0	0
(34, 149, 19, 13)	(155, 43)	[	0.9031564997511682	1.0	0
(43, 164, 1, 13)	(170, 43)	-	0.9600319616511285	1.0	0
(40, 178, 8, 8)	(182, 44)	[	0.9031564997511682	1.0	0
(34, 187, 19, 6)	(190, 43)	)	0.965506986283583	1.0	0
(41, 196, 19, 21)	(204, 49)	C	0.9512340150905829	1.0	0
(39, 219, 28, 7)	(221, 52)	(	0.965506986283583	1.0	0
(48, 228, 12, 11)	(233, 53)	s	0.9415793762163014	1.0	0
(39, 241, 28, 7)	(245, 53)	)	0.975609756097561	1.0	0
(39, 258, 28, 2)	(258, 52)	|	1.0	1.0	0
(48, 263, 12, 14)	(270, 54)	x	0.9487347984148984	1.0	0
(39, 280, 28, 7)	(282, 52)	(	0.965506986283583	1.0	0
(48, 289, 12, 11)	(294, 53)	s	0.9415793762163014	1.0	0
(39, 302, 28, 7)	(306, 53)	)	0.965506986283583	1.0	0
(39, 314, 28, 2)	(314, 52)	|	1.0	1.0	0
(41, 324, 19, 26)	(336, 52)	[	0.9031564997511682	1.0	0
(42, 360, 22, 18)	(369, 53)	\leq	0.9507484766422147	1.0	0
(75, 387, 8, 9)	(391, 79)	|	0.926829268292683	1.0	0
(73, 397, 11, 11)	(401, 78)	\in	0.935981560033552	1.0	3
(48, 398, 12, 10)	(402, 54)	\mathbb{S}	0.9365255258878067	1.0	3
(69, 411, 19, 10)	(415, 77)	[	0.9031564997511682	1.0	4
(48, 409, 12, 14)	(416, 54)	\text{u}	0.9275000566405587	1.0	4
(76, 422, 10, 8)	(425, 80)	|	0.926829268292683	1.0	0
(48, 423, 17, 15)	(429, 55)	\text{p}	0.9390289239150308	1.0	0
(81, 432, 6, 4)	(434, 83)	,	0.9172394111397633	1.0	0
(71, 437, 12, 6)	(439, 77)	[	0.9031564997511682	1.0	0
(69, 443, 19, 4)	(445, 78)	]	0.975789124937792	1.0	0
(39, 456, 28, 2)	(456, 52)	|	1.0	1.0	0
(48, 461, 12, 15)	(468, 54)	x	0.9487347984148984	1.0	0
(39, 479, 28, 7)	(481, 53)	(	0.965506986283583	1.0	0
(48, 487, 12, 12)	(493, 54)	s	0.9415793762163014	1.0	0
(39, 501, 28, 7)	(505, 53)	)	0.975609756097561	1.0	0
(39, 513, 28, 2)	(514, 52)	|	1.0	1.0	0
(79, 525, 13, 10)	(529, 86)	k	0.9171329209534959	1.0	0
(12, 523, 60, 38)	(540, 46)	[	0.9031564997511682	1.0	0
(79, 536, 13, 24)	(551, 86)	]	0.9031564997511682	1.0	0
(48, 567, 12, 11)	(572, 53)	e	0.9586903807613987	1.0	0
(43, 580, 1, 13)	(586, 43)	-	0.9600319616511285	1.0	0
(40, 594, 8, 12)	(600, 44)	|	0.926829268292683	1.0	0
(35, 607, 13, 10)	(611, 42)	k	0.9073517890775841	1.0	0
(22, 624, 62, 26)	(637, 56)	[	0.9031564997511682	1.0	0
(79, 646, 1, 13)	(652, 79)	-	0.9600319616511285	1.0	3
(17, 651, 12, 6)	(653, 23)	[	0.9031564997511682	1.0	3
(24, 659, 1, 13)	(665, 24)	-	0.9600319616511285	1.0	3
(71, 661, 13, 10)	(665, 78)	k	0.9171329209534959	1.0	3
(16, 673, 13, 10)	(677, 23)	k	0.9073517890775841	1.0	3
(79, 672, 1, 13)	(678, 79)	-	0.9600319616511285	1.0	3
(71, 688, 13, 7)	(690, 78)	[	0.951578249875584	1.0	0
(41, 702, 19, 21)	(711, 49)	C	0.9512340150905829	1.0	0
(39, 725, 28, 29)	(739, 53)	|	0.926829268292683	1.0	0
(41, 762, 19, 25)	(773, 52)	[	0.9031564997511682	1.0	0

Case03-H
Time: 28.05043387413025

Position (y, x, h, w)	Centroid (x, y)	Answer	Similarity	2nd Similarity	Depth
(22, 69, 61, 25)	(81, 52)	\measuredangle	0.8944180840124287	1.0	0
(73, 84, 11, 5)	(86, 78)	t	0.9301569704230421	1.0	0
(77, 91, 10, 3)	(92, 82)	(	0.9454617566463466	1.0	0
(77, 95, 10, 3)	(96, 82)	)	0.926829268292683	1.0	0
(18, 96, 11, 5)	(98, 23)	[	0.9031564997511682	1.0	0
(48, 109, 12, 10)	(113, 53)	e	0.9173807615227972	1.0	0
(43, 122, 1, 12)	(128, 43)	-	0.9600319616511285	1.0	0
(40, 136, 8, 11)	(141, 44)	\alpha	0.9250468311004139	1.0	0
(35, 150, 17, 4)	(151, 43)	(	0.9512195121951219	1.0	1
(37, 156, 11, 6)	(158, 42)	t	0.9506135201675205	1.0	1
(43, 164, 1, 12)	(170, 43)	-	0.9600319616511285	1.0	0
(40, 179, 8, 7)	(182, 43)	S	0.9042173714778848	1.0	0
(34, 188, 18, 4)	(190, 42)	)	0.9512195121951219	1.0	0
(41, 197, 19, 14)	(201, 50)	[	0.9127064485393568	1.0	0
(53, 208, 6, 5)	(210, 56)	/	0.9083782583297247	1.0	2
(41, 212, 7, 4)	(214, 44)	[	0.8917256751322972	1.0	2
(40, 219, 26, 6)	(221, 53)	(	0.975609756097561	1.0	1

(48, 228, 12, 11)	(234, 54)	s	0.9586903807613987	1.0	0
(40, 241, 27, 7)	(245, 52)	)	0.965506986283583	1.0	0
(40, 258, 27, 1)	(258, 53)	|	1.0	1.0	0
(50, 264, 2, 2)	(264, 50)	[	0.9031564997511682	1.0	3
(57, 263, 3, 4)	(264, 58)	|	0.926829268292683	1.0	3
(48, 267, 12, 6)	(270, 54)	[	0.9273673748133762	1.0	0
(56, 274, 2, 2)	(274, 56)	[	0.9031564997511682	1.0	3
(48, 273, 3, 4)	(275, 49)	[	0.9031564997511682	1.0	3
(40, 280, 26, 6)	(282, 53)	(	0.975609756097561	1.0	0
(48, 289, 12, 11)	(295, 54)	s	0.9586903807613987	1.0	0
(40, 303, 27, 6)	(306, 53)	)	0.975609756097561	1.0	0
(40, 315, 27, 1)	(315, 53)	|	1.0	1.0	0
(41, 325, 19, 13)	(331, 51)	d	0.9423130255462239	1.0	1
(56, 336, 3, 5)	(338, 57)	[	0.9031564997511682	1.0	1
(48, 341, 12, 8)	(345, 53)	[	0.9031564997511682	1.0	1
(43, 360, 21, 17)	(369, 54)	\leq	0.9753742383211074	1.0	0
(75, 388, 8, 7)	(392, 79)	s	0.9076288832578542	1.0	0
(48, 399, 12, 8)	(402, 55)	[	0.9031564997511682	1.0	0
(73, 398, 11, 9)	(402, 78)	\in	0.9547321269787408	1.0	0
(48, 404, 4, 3)	(406, 49)	[	0.9031564997511682	1.0	0
(69, 411, 19, 3)	(411, 78)	[	0.975789124937792	1.0	4
(48, 409, 12, 8)	(412, 53)	[	0.9273673748133762	1.0	4
(72, 415, 11, 6)	(417, 77)	t	0.9506135201675205	1.0	3
(48, 417, 12, 6)	(419, 54)	[	0.951578249875584	1.0	3
(76, 422, 10, 3)	(423, 80)	(	0.926829268292683	1.0	0
(76, 426, 10, 3)	(427, 80)	)	0.9454617566463466	1.0	3
(48, 424, 17, 13)	(429, 55)	\text{p}	0.9568869386440774	1.0	3
(81, 433, 6, 2)	(434, 83)	[	0.9031564997511682	1.0	0
(72, 437, 11, 6)	(439, 77)	t	0.9506135201675205	1.0	0
(69, 444, 19, 3)	(446, 78)	]	0.975789124937792	1.0	0
(40, 457, 27, 1)	(457, 53)	|	1.0	1.0	0
(48, 462, 12, 13)	(468, 54)	x	0.9487347984148984	1.0	0
(40, 479, 27, 6)	(481, 53)	(	0.965506986283583	1.0	0
(48, 488, 12, 10)	(493, 54)	s	0.9415793762163014	1.0	0
(40, 501, 27, 6)	(505, 53)	)	0.9512195121951219	1.0	0
(40, 513, 27, 1)	(513, 53)	|	1.0	1.0	0
(79, 525, 13, 9)	(529, 86)	k	0.9344878217919581	1.0	0
(33, 524, 38, 36)	(539, 52)	\sum	0.9872639880016522	1.0	4
(12, 535, 13, 12)	(541, 18)	]	0.9273673748133762	1.0	4
(85, 536, 5, 13)	(542, 87)	=	0.9648635815536847	1.0	0
(12, 546, 5, 4)	(547, 13)	[	0.9031564997511682	1.0	0
(79, 551, 13, 8)	(555, 85)	0	0.9568267108223655	1.0	0
(49, 568, 11, 6)	(570, 54)	[	0.9273673748133762	1.0	0
(48, 573, 5, 5)	(575, 49)	]	0.9031564997511682	1.0	3
(58, 575, 1, 1)	(575, 58)	\blacksquare	0.9738108599560538	1.0	3
(57, 577, 1, 1)	(577, 57)	\blacksquare	0.9738108599560538	1.0	3
(43, 581, 1, 12)	(586, 43)	-	0.9600319616511285	1.0	0
(40, 595, 8, 10)	(599, 44)	|	0.926829268292683	1.0	0
(41, 605, 1, 1)	(605, 41)	\blacksquare	0.9738108599560538	1.0	0
(35, 608, 13, 9)	(611, 42)	k	0.9171329209534959	1.0	0
(22, 624, 61, 25)	(637, 52)	j	0.8876688087396539	1.0	5
(73, 639, 11, 5)	(641, 78)	[	0.9031564997511682	1.0	5
(79, 647, 1, 12)	(652, 79)	-	0.9600319616511285	1.0	3
(18, 651, 11, 6)	(653, 23)	t	0.9506135201675205	1.0	3
(24, 659, 1, 12)	(664, 24)	-	0.9600319616511285	1.0	3
(71, 662, 13, 8)	(665, 78)	k	0.9344878217919581	1.0	3
(16, 674, 13, 9)	(677, 23)	[	0.9031564997511682	1.0	0
(79, 673, 1, 12)	(678, 79)	-	0.9600319616511285	1.0	0
(71, 688, 13, 6)	(690, 78)	1	0.9332591355734	1.0	0
(41, 703, 19, 19)	(710, 49)	C	0.9512340150905829	1.0	0
(40, 726, 27, 6)	(727, 53)	(	0.9512195121951219	1.0	0
(48, 735, 12, 10)	(740, 53)	s	0.9586903807613987	1.0	0
(40, 748, 27, 6)	(751, 53)	)	0.975609756097561	1.0	0
(41, 762, 19, 13)	(769, 52)	d	0.9592091491775998	1.0	1
(48, 776, 12, 11)	(782, 54)	s	0.9586903807613987	1.0	1

Case05-H
Time: 5.334937572479248

Position (y, x, h, w)	Centroid (x, y)	Answer	Similarity	2nd Similarity	Depth
(94, 4, 72, 34)	(24, 135)	j	0.9508823327587399	1.0	0
(94, 46, 56, 23)	(58, 126)	i	0.9524348505845506	1.0	0
(94, 75, 56, 23)	(87, 126)	i	0.9524348505845506	1.0	0
(94, 103, 56, 23)	(115, 126)	i	0.9524348505845506	1.0	0
(124, 155, 9, 9)	(159, 128)	|	0.926829268292683	1.0	0
(2, 219, 51, 26)	(234, 32)	j	0.9450847785761639	1.0	6
(208, 226, 40, 18)	(235, 231)	i	0.9663663603001844	1.0	6
(70, 194, 117, 111)	(242, 130)	\sum	0.9872639880016522	1.0	6
(208, 246, 51, 26)	(261, 238)	j	0.9644777583337306	1.0	6
(2, 250, 51, 26)	(265, 32)	j	0.9450847785761639	1.0	6
(94, 323, 72, 34)	(343, 135)	j	0.9508823327587399	1.0	1
(124, 388, 9, 9)	(392, 128)	|	0.926829268292683	1.0	1
(70, 426, 117, 111)	(474, 130)	\sum	0.9872639880016522	1.0	4
(6, 474, 40, 18)	(483, 29)	i	0.9538979554442426	1.0	4

Chamfer Similarity

Similarity Threshold = 0.985

Case01-C
Time: 0.4013533592224121

Position (y, x, h, w)	Centroid (x, y)	Answer	Similarity	2nd Similarity	Depth

Figure 14: Case 01, Chamfer

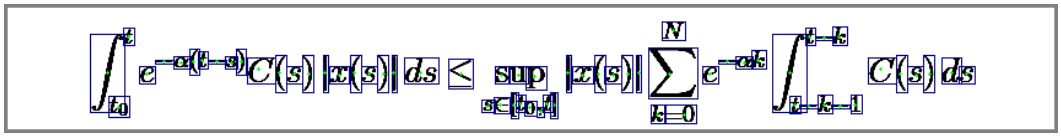

Figure 15: Case 02, Chamfer

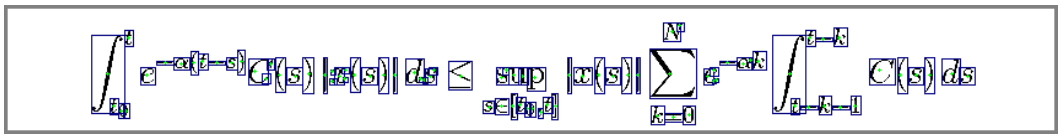

Figure 16: Case 03, Chamfer

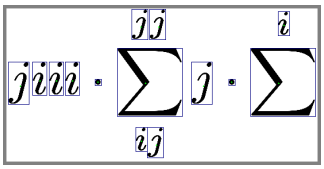

Figure 17: Case 05, Chamfer

```
+----------------------+-----------------+-------+--------------------+-----------------+-------+
|     (12, 2, 12, 7)   |     (5, 18)     |   t   | 0.9923610632462397 |       1.0       |   0   |
+----------------------+-----------------+-------+--------------------+-----------------+-------+

Case02-C
Time: 24.83780837059021
+----------------------+-----------------+--------------------+--------------------+-----------------+-------+
| Position (y, x, h, w) | Centroid (x, y) |       Answer       |     Similarity     | 2nd Similarity | Depth |
+----------------------+-----------------+--------------------+--------------------+-----------------+-------+
|    (22, 68, 61, 26)  |    (81, 52)     |        \int        | 0.9843964497850461 |       1.0       |   0   |
|    (72, 83, 15, 15)  |    (90, 80)     | \Longleftrightarrow | 0.981457787252258  |       1.0       |   0   |
|    (17, 95, 12, 7)   |    (98, 23)     |         t          | 0.9921126269600911 |       1.0       |   0   |
|   (48, 108, 12, 11)  |   (113, 53)     |         e          | 0.9908783116139559 |       1.0       |   0   |
|    (43, 121, 1, 13)  |   (127, 43)     |         -          | 0.9992313838779063 |       1.0       |   0   |
|    (40, 136, 8, 12)  |   (141, 44)     |       \alpha       | 0.9910398216021798 |       1.0       |   0   |
|    (34, 149, 19, 6)  |   (151, 43)     |         (          | 0.9948141402412572 |       1.0       |   1   |
|    (36, 156, 12, 6)  |   (158, 42)     |         t          | 0.9896422086331647 |       1.0       |   1   |
|    (43, 164, 1, 13)  |   (170, 43)     |         -          | 0.9992313838779063 |       1.0       |   0   |
|    (40, 178, 8, 8)   |   (182, 44)     |    \blacksquare    | 0.9875261559844912 |       1.0       |   0   |
|    (34, 187, 19, 6)  |   (190, 43)     |         )          | 0.9959876646805674 |       1.0       |   0   |
|   (41, 196, 19, 21)  |   (204, 49)     |         C          | 0.995805424297517  |       1.0       |   0   |
|    (39, 219, 28, 7)  |   (221, 52)     |         (          | 0.9967567599842723 |       1.0       |   0   |
|   (48, 228, 12, 11)  |   (233, 53)     |         s          | 0.9933883954603301 |       1.0       |   0   |
|    (39, 241, 28, 7)  |   (245, 53)     |         )          | 0.9965447154471545 |       1.0       |   0   |
|    (39, 258, 28, 2)  |   (258, 52)     |         \|         |        1.0         |       1.0       |   0   |
|   (48, 263, 12, 14)  |   (270, 54)     |         x          | 0.9928938404667408 |       1.0       |   0   |
|    (39, 280, 28, 7)  |   (282, 52)     |         (          | 0.9967567599842723 |       1.0       |   0   |
|   (48, 289, 12, 11)  |   (294, 53)     |         s          | 0.9933883954603301 |       1.0       |   0   |
|    (39, 302, 28, 7)  |   (306, 53)     |         )          | 0.9957599028410242 |       1.0       |   0   |
|    (39, 314, 28, 2)  |   (314, 52)     |         \|         |        1.0         |       1.0       |   0   |
|   (41, 324, 19, 26)  |   (336, 52)     |     \spadesuit     | 0.9811565973823416 |       1.0       |   0   |
|   (42, 360, 22, 18)  |   (369, 53)     |        \leq        | 0.9959994064275194 |       1.0       |   0   |
|    (75, 387, 8, 9)   |   (391, 79)     |         s          | 0.9900540300436511 |       1.0       |   0   |
|   (73, 397, 11, 11)  |   (401, 78)     |        \in         | 0.9934666966190748 |       1.0       |   3   |
|   (48, 398, 12, 10)  |   (402, 54)     |      \text{s}      | 0.9937478041110738 |       1.0       |   3   |
|    (69, 411, 19, 4)  |   (412, 78)     |         [          | 0.9964292571306377 |       1.0       |   5   |
|   (48, 409, 12, 14)  |   (416, 54)     |      \text{u}      | 0.9943956766930595 |       1.0       |   4   |
|    (71, 415, 12, 6)  |   (417, 77)     |         t          | 0.9896422086331647 |       1.0       |   5   |
|    (76, 422, 10, 8)  |   (425, 80)     |         0          | 0.9900524245194917 |       1.0       |   0   |
|   (48, 423, 17, 15)  |   (429, 55)     |      \text{p}      | 0.9944387979631886 |       1.0       |   0   |
|    (81, 432, 6, 4)   |   (434, 83)     |         ,          | 0.9841207325438895 |       1.0       |   0   |
|    (71, 437, 12, 6)  |   (439, 77)     |         t          | 0.9896422086331647 |       1.0       |   0   |
|    (69, 443, 19, 4)  |   (445, 78)     |         ]          | 0.9963140330916971 |       1.0       |   0   |
|    (39, 456, 28, 2)  |   (456, 52)     |         \|         |        1.0         |       1.0       |   0   |
|   (48, 461, 12, 15)  |   (468, 54)     |         x          | 0.9914043311641592 |       1.0       |   0   |
|    (39, 479, 28, 7)  |   (481, 53)     |         (          | 0.9957811825840156 |       1.0       |   0   |
```

(48, 487, 12, 12)	(493, 54)	s	0.9933296085389572	1.0	0
(39, 501, 28, 7)	(505, 53)	)	0.9957317073170732	1.0	0
(39, 513, 28, 2)	(514, 52)	|	1.0	1.0	0
(79, 525, 13, 10)	(529, 86)	k	0.9914993350993432	1.0	0
(33, 523, 39, 38)	(539, 53)	\sum	0.998658112181978	1.0	4
(12, 534, 13, 17)	(542, 18)	N	0.9946213637233691	1.0	4
(79, 536, 13, 24)	(551, 86)	\nexists	0.9752251239517647	1.0	0
(48, 567, 12, 11)	(572, 53)	e	0.9922950538951848	1.0	0
(43, 580, 1, 13)	(586, 43)	-	0.9992313838779063	1.0	0
(40, 594, 8, 12)	(600, 44)	\alpha	0.9886884936849081	1.0	0
(35, 607, 13, 10)	(611, 42)	k	0.9889372487970257	1.0	0
(22, 624, 61, 26)	(637, 52)	\int	0.9885723120281471	1.0	5
(72, 638, 12, 7)	(641, 78)	t	0.9892324905733441	1.0	5
(79, 646, 1, 13)	(652, 79)	-	0.9992313838779063	1.0	3
(17, 651, 12, 6)	(653, 23)	t	0.9896422086331647	1.0	3
(24, 659, 1, 13)	(665, 24)	-	0.9992313838779063	1.0	3
(71, 661, 13, 10)	(665, 78)	k	0.9912248189224879	1.0	3
(16, 673, 13, 10)	(677, 23)	k	0.9889372487970257	1.0	3
(79, 672, 1, 13)	(678, 79)	-	0.9992313838779063	1.0	3
(71, 688, 13, 7)	(690, 78)	1	0.994792254413714	1.0	0
(41, 702, 19, 21)	(711, 49)	C	0.9956743529854594	1.0	0
(39, 725, 28, 7)	(727, 53)	(	0.9966659058301813	1.0	1
(48, 734, 12, 11)	(740, 54)	s	0.9910415333317126	1.0	1
(39, 747, 28, 7)	(751, 53)	)	0.9957599028410242	1.0	1
(41, 762, 19, 14)	(769, 52)	d	0.9905639624998505	1.0	1
(48, 776, 12, 11)	(781, 53)	s	0.9933883954603301	1.0	1

Case03-C
Time: 35.45501756668091

Position (y, x, h, w)	Centroid (x, y)	Answer	Similarity	2nd Similarity	Depth
(22, 69, 61, 25)	(81, 52)	\int	0.9883786243395991	1.0	0
(73, 84, 11, 5)	(86, 78)	t	0.9908967547796858	1.0	0
(77, 91, 10, 3)	(92, 82)	(	0.9925631954742102	1.0	0
(77, 95, 10, 3)	(96, 82)	)	0.9895428311988358	1.0	0
(18, 96, 11, 5)	(98, 23)	t	0.9927942493233284	1.0	0
(48, 109, 12, 10)	(113, 53)	e	0.9897676440159678	1.0	0
(43, 122, 1, 12)	(128, 43)	-	0.9992313838779063	1.0	0
(40, 136, 8, 11)	(141, 44)	\alpha	0.99303619593157	1.0	0
(35, 150, 17, 4)	(151, 43)	(	0.9937868042911754	1.0	1
(37, 156, 11, 6)	(158, 42)	t	0.9957962301081443	1.0	1
(43, 164, 1, 12)	(170, 43)	-	0.9992313838779063	1.0	0
(40, 179, 8, 7)	(182, 43)	S	0.9899047818161499	1.0	0
(34, 188, 18, 4)	(190, 42)	)	0.9937227886975715	1.0	0
(41, 197, 19, 14)	(201, 50)	[	0.9893225427911496	1.0	0
(53, 208, 6, 5)	(210, 56)	/	0.9844607344397801	1.0	2
(41, 212, 7, 4)	(214, 44)	\forall	0.9802874960493051	1.0	2
(40, 219, 26, 6)	(221, 53)	(	0.9967825635703166	1.0	1
(48, 228, 12, 11)	(234, 54)	s	0.9922013616016846	1.0	0
(40, 241, 27, 7)	(245, 52)	)	0.995364921764024	1.0	0
(40, 258, 27, 1)	(258, 53)	|	1.0	1.0	0
(50, 264, 2, 2)	(264, 50)	l	0.9815581988890082	1.0	3
(57, 263, 3, 4)	(264, 58)	\clubsuit	0.9893381633556091	1.0	3
(48, 267, 12, 6)	(270, 54)	\text{l}	0.9873673014222473	1.0	0
(56, 274, 2, 2)	(274, 56)	l	0.981686520054095	1.0	3
(48, 273, 3, 4)	(275, 49)	\text{l}	0.9845801240459233	1.0	3
(40, 280, 26, 6)	(282, 53)	(	0.9967825635703166	1.0	0
(48, 289, 12, 11)	(295, 54)	s	0.9922013616016846	1.0	0
(40, 303, 27, 6)	(306, 53)	)	0.9959525569281666	1.0	0
(40, 315, 27, 1)	(315, 53)	|	1.0	1.0	0
(41, 325, 19, 13)	(331, 51)	d	0.9899744201348628	1.0	1
(56, 336, 2, 1)	(336, 56)	\blacksquare	0.9999832977423189	1.0	2
(56, 339, 3, 2)	(339, 57)	\blacksquare	0.9902589804401682	1.0	2
(49, 341, 11, 7)	(344, 54)	\text{S}	0.9833875848535063	1.0	2
(48, 344, 4, 5)	(347, 49)	]	0.9840414706067209	1.0	2
(43, 360, 21, 17)	(369, 54)	\leq	0.9954949139867582	1.0	0
(75, 388, 8, 7)	(392, 79)	\mathcal{S}	0.9892400039356637	1.0	0
(48, 399, 12, 8)	(402, 55)	\text{S}	0.9920420366630727	1.0	0
(73, 398, 11, 9)	(402, 78)	\in	0.9940084501155451	1.0	0
(48, 404, 4, 3)	(406, 49)	]	0.987870689488328	1.0	0
(69, 411, 19, 3)	(411, 78)	[	0.9995252769595645	1.0	4
(48, 409, 12, 8)	(412, 53)	\text{l}	0.9850117226070044	1.0	4
(72, 415, 11, 6)	(417, 77)	t	0.9957962301081443	1.0	3
(48, 417, 12, 6)	(419, 54)	\text{l}	0.9966527637385253	1.0	3
(76, 422, 10, 3)	(423, 80)	(	0.9906642349315147	1.0	0
(76, 426, 10, 3)	(427, 80)	)	0.9936674013954355	1.0	3
(48, 424, 17, 13)	(429, 55)	\text{p}	0.9930845840591124	1.0	3
(81, 433, 6, 2)	(434, 83)	]	0.9840903722807557	1.0	0
(72, 437, 11, 6)	(439, 77)	t	0.9957962301081443	1.0	0
(69, 444, 19, 3)	(446, 78)	]	0.9994100529206239	1.0	0
(40, 457, 27, 1)	(457, 53)	|	1.0	1.0	0
(48, 462, 12, 13)	(468, 54)	x	0.9922149011216916	1.0	0
(40, 479, 27, 6)	(481, 53)	(	0.9956595281964926	1.0	0
(48, 488, 12, 10)	(493, 54)	\mathcal{S}	0.9913228951052659	1.0	0
(40, 501, 27, 6)	(505, 53)	)	0.9903943980498564	1.0	0
(40, 513, 27, 1)	(513, 53)	|	1.0	1.0	0
(79, 525, 13, 9)	(529, 86)	k	0.9906948865260685	1.0	0
(33, 524, 38, 36)	(539, 52)	\sum	0.9990485637547387	1.0	4
(12, 535, 13, 12)	(541, 18)	]	0.982245433104974	1.0	4
(85, 536, 5, 13)	(542, 87)	=	0.9993725639563158	1.0	0
(12, 546, 5, 4)	(547, 13)	\mathcal{T}	0.9869863512645882	1.0	0
(79, 551, 13, 8)	(555, 85)	0	0.9959163513438614	1.0	0
(49, 568, 11, 6)	(570, 54)	[	0.9888797031209026	1.0	0
(48, 573, 5, 5)	(575, 49)	)	0.9816929539404685	1.0	3
(58, 575, 1, 1)	(575, 58)	\blacksquare	0.9999832977423189	1.0	3
(57, 577, 1, 1)	(577, 57)	\blacksquare	0.9999832977423189	1.0	3
(43, 581, 1, 12)	(586, 43)	-	0.9992313838779063	1.0	0
(40, 595, 8, 10)	(599, 44)	\alpha	0.9867632079330648	1.0	0
(41, 605, 1, 1)	(605, 41)	\blacksquare	0.9999832977423189	1.0	0
(35, 608, 13, 9)	(611, 42)	k	0.990344093222219	1.0	0

(22, 624, 61, 25)	(637, 52)	\int	0.9902707355440981	1.0	5
(73, 639, 11, 5)	(641, 78)	t	0.9912331975986025	1.0	5
(79, 647, 1, 12)	(652, 79)	-	0.9992313838779063	1.0	3
(18, 651, 11, 6)	(653, 23)	t	0.9957962301081443	1.0	3
(24, 659, 1, 12)	(664, 24)	-	0.9992313838779063	1.0	3
(71, 662, 13, 8)	(665, 78)	k	0.9912058683379049	1.0	3
(16, 674, 13, 9)	(677, 23)	k	0.9905569125545978	1.0	0
(79, 673, 1, 12)	(678, 79)	-	0.9992313838779063	1.0	0
(71, 688, 13, 6)	(690, 78)	1	0.996662620238981	1.0	0
(41, 703, 19, 19)	(710, 49)	C	0.9958234213695515	1.0	0
(40, 726, 27, 6)	(727, 53)	(	0.9892720520776794	1.0	0
(48, 735, 12, 10)	(740, 53)	s	0.9919630630220068	1.0	0
(40, 748, 27, 6)	(751, 53)	)	0.9959525569281666	1.0	0
(41, 762, 19, 13)	(769, 52)	d	0.9947517843313528	1.0	1
(48, 776, 12, 11)	(782, 54)	s	0.9922013616016846	1.0	1

Case05-C
Time: 6.61948561668396

Position (y, x, h, w)	Centroid (x, y)	Answer	Similarity	2nd Similarity	Depth
(94, 4, 72, 34)	(24, 135)	j	0.99551625275265	1.0	0
(94, 46, 56, 23)	(58, 126)	i	0.9963112358651984	1.0	0
(94, 75, 56, 23)	(87, 126)	i	0.9963112358651984	1.0	0
(94, 103, 56, 23)	(115, 126)	i	0.9963112358651984	1.0	0
(124, 155, 9, 9)	(159, 128)	\blacksquare	0.9951500088011779	1.0	0
(2, 219, 51, 26)	(234, 32)	j	0.9935345547958635	1.0	6
(208, 226, 40, 18)	(235, 231)	i	0.9974068196341481	1.0	6
(70, 194, 117, 111)	(242, 130)	\sum	0.9995812486844352	1.0	6
(208, 246, 51, 26)	(261, 238)	j	0.9971845797330895	1.0	6
(2, 250, 51, 26)	(265, 32)	j	0.9940586988316582	1.0	6
(94, 323, 72, 34)	(343, 135)	j	0.99551625275265	1.0	1
(124, 388, 9, 9)	(392, 128)	\blacksquare	0.9951500088011779	1.0	1
(70, 426, 117, 111)	(474, 130)	\sum	0.9995812486844352	1.0	4
(6, 474, 40, 18)	(483, 29)	i	0.9936281130702643	1.0	4

L2 Pixelwise Similarity + Hausdorff recheck

Similarity Threshold = 0.7; Second Similarity Threshold = 0.9

Figure 18: Case 01, L2 + Hausdorff

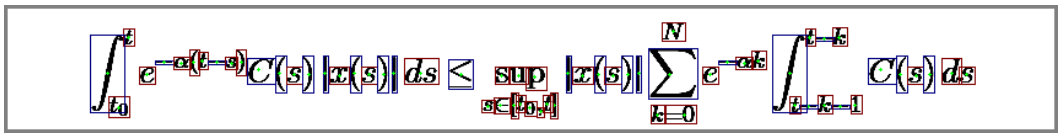

Figure 19: Case 02, L2 + Hausdorff

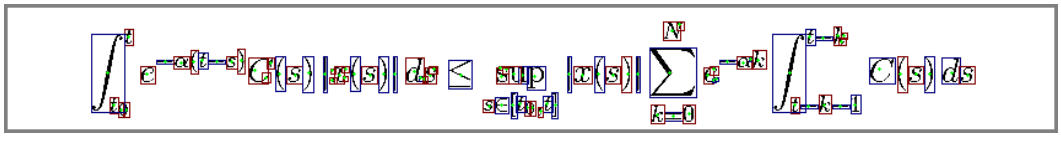

Figure 20: Case 03, L2 + Hausdorff

Case01-L2-H
Time: 0.05126070976257324

Position (y, x, h, w)	Centroid (x, y)	Answer	Similarity	2nd Similarity	Depth
(12, 2, 12, 7)	(5, 18)	t	0.6501996994903936	0.9301569704230421	0

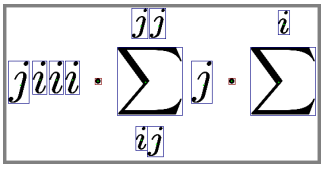

Figure 21: Case 05, L2 + Hausdorff

Case02-L2-H
Time: 1.8391032218933105

Position (y, x, h, w)	Centroid (x, y)	Answer	Similarity	2nd Similarity	Depth
(22, 68, 61, 26)	(81, 52)	\int	0.8112695466053161	0.7511643486715837	0
(72, 83, 15, 15)	(90, 80)	\text{k}	0.48111248463144873	0.8130922745936009	0
(17, 95, 12, 7)	(98, 23)	t	0.6412090482077021	0.9301569704230421	0
(48, 108, 12, 11)	(113, 53)	c	0.6302641111334014	0.7934519038069932	0
(43, 121, 1, 13)	(127, 43)	-	0.8007422116349886	0.9600319616511285	0
(40, 136, 8, 12)	(141, 44)	\alpha	0.5636751742760288	0.9250468311004139	0
(34, 149, 19, 6)	(151, 43)	(	0.6800281140816784	0.9512195121951219	1
(36, 156, 12, 6)	(158, 42)	t	0.5509637992098394	0.9012270403350411	1
(43, 164, 1, 13)	(170, 43)	-	0.8007422116349886	0.9600319616511285	0
(40, 178, 8, 8)	(182, 44)	\cdot	0.5336386048560049	0.8232233047033631	0
(34, 187, 19, 6)	(190, 43)	)	0.6984232397013816	0.965506986283583	0
(41, 196, 19, 21)	(204, 49)	C	0.7489220313776552	0.9512340150905829	0
(39, 219, 28, 7)	(221, 52)	(	0.7395491111297813	0.965506986283583	0
(48, 228, 12, 11)	(233, 53)	s	0.6442742711748131	0.9415793762163014	0
(39, 241, 28, 7)	(245, 53)	)	0.7257545814123264	0.975609756097561	0
(39, 258, 28, 2)	(258, 52)	|	1.0	1.0	0
(48, 263, 12, 14)	(270, 54)	x	0.616991876571773	0.9487347984148984	0
(39, 280, 28, 7)	(282, 52)	(	0.7395491111297813	0.965506986283583	0
(48, 289, 12, 11)	(294, 53)	s	0.6442742711748131	0.9415793762163014	0
(39, 302, 28, 7)	(306, 53)	)	0.7208980172688736	0.965506986283583	0
(39, 314, 28, 2)	(314, 52)	|	0.972294003887706	1.0	0
(41, 324, 19, 26)	(336, 52)	L	0.5090748163863589	0.7852163681360275	0
(42, 360, 22, 18)	(369, 53)	\leq	0.785439400295016	0.9507484766422147	0
(75, 387, 8, 9)	(391, 79)	s	0.5725621765910893	0.9173807615227972	0
(73, 397, 11, 11)	(401, 78)	\in	0.6917619024564499	0.935981560033552	3
(48, 398, 12, 10)	(402, 54)	\text{s}	0.6458485552135702	0.9131255514473862	3
(69, 411, 19, 4)	(412, 78)	[	0.6489462442853158	0.975789124937792	5
(48, 409, 12, 14)	(416, 54)	\text{n}	0.627418862649586	0.8660007421476806	4
(71, 415, 12, 6)	(417, 77)	t	0.5509637992098394	0.9012270403350411	5
(76, 422, 10, 8)	(425, 80)	0	0.55120206820204	0.9084156233691004	0
(48, 423, 17, 15)	(429, 55)	\text{p}	0.6809162258061873	0.9390289239150308	0
(81, 432, 6, 4)	(434, 83)	,	0.5989129648050695	0.9172394111397633	0
(71, 437, 12, 6)	(439, 77)	t	0.5509637992098394	0.9012270403350411	0
(69, 443, 19, 4)	(445, 78)	]	0.6462592496082983	0.975789124937792	0
(39, 456, 28, 2)	(456, 52)	|	0.972294003887706	1.0	0
(48, 461, 12, 15)	(468, 54)	x	0.630689683546971	0.9487347984148984	0
(39, 479, 28, 7)	(481, 53)	(	0.7126966312204062	0.965506986283583	0
(48, 487, 12, 12)	(493, 54)	s	0.6599998354065117	0.9415793762163014	0
(39, 501, 28, 7)	(505, 53)	)	0.7120520177480982	0.975609756097561	0
(39, 513, 28, 2)	(514, 52)	|	1.0	1.0	0
(79, 525, 13, 10)	(529, 86)	k	0.5758825872966433	0.9171329209534959	0
(33, 523, 39, 38)	(539, 53)	\sum	0.8047063556258368	0.9715214114094413	4
(12, 534, 13, 17)	(542, 18)	N	0.6546182481105398	0.9357838700932064	4
(79, 536, 13, 24)	(551, 86)	\longrightarrow	0.5455451124910109	0.8584212465450973	0
(48, 567, 12, 11)	(572, 53)	c	0.6359622330989851	0.7934519038069932	0
(43, 580, 1, 13)	(586, 43)	-	0.8007422116349886	0.9600319616511285	0
(40, 594, 8, 12)	(600, 44)	\alpha	0.5101686826599887	0.8994397715269014	0
(35, 607, 13, 10)	(611, 42)	k	0.5457637879691819	0.9073517890775841	0
(22, 624, 61, 26)	(637, 52)	\int	0.8481457206272577	0.7543316689271135	5
(72, 638, 12, 7)	(641, 78)	t	0.5944584485237567	0.921913119055697	5
(79, 646, 1, 13)	(652, 79)	-	0.8007422116349886	0.9600319616511285	3
(17, 651, 12, 6)	(653, 23)	t	0.5509637992098394	0.9012270403350411	3
(24, 659, 1, 13)	(665, 24)	-	0.8007422116349886	0.9600319616511285	3
(71, 661, 13, 10)	(665, 78)	k	0.5730413840756658	0.9171329209534959	3
(16, 673, 13, 10)	(677, 23)	k	0.5457637879691819	0.9073517890775841	3
(79, 672, 1, 13)	(678, 79)	-	0.8007422116349886	0.9600319616511285	3
(71, 688, 13, 7)	(690, 78)	\text{l}	0.662755472202137	0.8979969398622931	0
(41, 702, 19, 21)	(711, 49)	C	0.7515082146139705	0.9512340150905829	0
(39, 725, 28, 7)	(727, 53)	(	0.7397297097623259	0.975609756097561	1
(48, 734, 12, 11)	(740, 54)	s	0.6045913594976304	0.9173807615227972	1
(39, 747, 28, 7)	(751, 53)	)	0.7208980172688736	0.965506986283583	1
(41, 762, 19, 14)	(769, 52)	d	0.5913285615589079	0.9355040018525315	1
(48, 776, 12, 11)	(781, 53)	s	0.6442742711748131	0.9415793762163014	1

Case03-L2-H
Time: 2.6358110904693604

Position (y, x, h, w)	Centroid (x, y)	Answer	Similarity	2nd Similarity	Depth
(22, 69, 61, 25)	(81, 52)	\int	0.8804873393286075	0.7640886364491144	0
(73, 84, 11, 5)	(86, 78)	t	0.6441517116959318	0.9301569704230421	0
(77, 91, 10, 3)	(92, 82)	(	0.6512793367097558	0.9454617566463466	0
(77, 95, 10, 3)	(96, 82)	\}	0.5426730137681869	0.8845914809673177	0
(18, 96, 11, 5)	(98, 23)	t	0.6471690877559237	0.9012270403350411	0
(48, 109, 12, 10)	(113, 53)	e	0.6560078584840772	0.9173807615227972	0
(43, 122, 1, 12)	(128, 43)	-	0.8007422116349886	0.9600319616511285	0
(40, 136, 8, 11)	(141, 44)	\alpha	0.6401934020661277	0.9250468311004139	0
(35, 150, 17, 4)	(151, 43)	(	0.6625122926824529	0.9512195121951219	1

(37, 156, 11, 6)	(158, 42)	t	0.7364316773540476	0.9506135201675205	1
(43, 164, 1, 12)	(170, 43)	-	0.8007422116349886	0.9600319616511285	0
(40, 179, 8, 7)	(182, 43)	S	0.5909722944389066	0.9042173714778848	0
(34, 188, 18, 4)	(190, 42)	)	0.6608101168813563	0.9512195121951219	0
(41, 197, 19, 14)	(201, 50)	\mathcal{C}	0.6502051924982701	0.7765676906088218	0
(53, 208, 6, 5)	(210, 56)	/	0.655018894273272	0.9083782583297247	2
(41, 212, 7, 4)	(214, 44)	\bigstar	0.4852629735258074	0.74287026138671	2
(40, 219, 26, 6)	(221, 53)	(	0.7892597890311289	0.975609756097561	1
(48, 228, 12, 11)	(234, 54)	s	0.6855544392543803	0.9586903807613987	0
(40, 241, 27, 7)	(245, 52)	)	0.7495430077581059	0.965506986283583	0
(40, 258, 27, 1)	(258, 53)	|	1.0	1.0	0
(50, 264, 2, 2)	(264, 50)	l	0.5325919575934173	0.8670355009370933	3
(57, 263, 3, 4)	(264, 58)	\cdot	0.574616268382353	0.8232233047033631	3
(48, 267, 12, 6)	(270, 54)	\text{l}	0.5866503869395692	0.8774075788064203	0
(56, 274, 2, 2)	(274, 56)	l	0.5333415253571769	0.8670355009370933	3
(48, 273, 3, 4)	(275, 49)	,	0.5552620223174003	0.8829588528038694	3
(40, 280, 26, 6)	(282, 53)	(	0.7892597890311289	0.975609756097561	0
(48, 289, 12, 11)	(295, 54)	s	0.6855544392543803	0.9586903807613987	0
(40, 303, 27, 6)	(306, 53)	)	0.761176477074688	0.975609756097561	0
(40, 315, 27, 1)	(315, 53)	|	1.0	1.0	0
(41, 325, 19, 13)	(331, 51)	d	0.6252310555453302	0.9423130255462239	1
(56, 336, 2, 1)	(336, 56)	\blacksquare	0.9267089330849527	0.9738108599560538	2
(56, 339, 3, 2)	(339, 57)	\blacksquare	0.6373230835302871	0.738108599560538	2
(49, 341, 11, 7)	(344, 54)	\text{S}	0.5349218701977737	0.7917625589419446	2
(48, 344, 4, 5)	(347, 49)	\daleth	0.5445688167622816	0.8487791748862477	2
(43, 360, 21, 17)	(369, 54)	\leq	0.7330452125125746	0.9753742383211074	0
(75, 388, 8, 7)	(392, 79)	\mathcal{S}	0.5956813076357885	0.8923144388422691	0
(48, 401, 1, 1)	(401, 48)	\blacksquare	0.6104547922684699	0.9738108599560538	3
(49, 399, 11, 8)	(402, 55)	\text{S}	0.5588301773506583	0.8215107648073812	3
(73, 398, 11, 9)	(402, 78)	\in	0.7280378688993686	0.9547321269787408	0
(48, 404, 4, 3)	(406, 49)	]	0.5875483375106125	0.9031564997511682	0
(69, 411, 19, 3)	(411, 78)	[	0.8584386780943228	0.975789124937792	4
(48, 409, 12, 8)	(412, 53)	\text{t}	0.622810586340846	0.7935937251538656	4
(72, 415, 11, 6)	(417, 77)	t	0.7364316773540476	0.9506135201675205	3
(48, 417, 12, 6)	(419, 54)	\text{l}	0.7602832897434025	0.8979969398622931	3
(76, 422, 10, 3)	(423, 80)	(	0.5447595728141809	0.926829268292683	0
(76, 426, 10, 3)	(427, 80)	)	0.6522993797258271	0.9454617566463466	3
(48, 424, 17, 13)	(429, 55)	\text{p}	0.7034994173092948	0.9568869386440774	3
(81, 433, 6, 2)	(434, 83)	,	0.553059929809641	0.8829588528038694	0
(72, 437, 11, 6)	(439, 77)	t	0.7364316773540476	0.9506135201675205	0
(69, 444, 19, 3)	(446, 78)	]	0.8557352334757056	0.975789124937792	0
(40, 457, 27, 1)	(457, 53)	|	1.0	1.0	0
(48, 462, 12, 13)	(468, 54)	x	0.6789572519240435	0.9487347984148984	0
(40, 479, 27, 6)	(481, 53)	(	0.7669114943388973	0.965506986283583	0
(48, 488, 12, 10)	(493, 54)	s	0.6567378325176901	0.9415793762163014	0
(40, 501, 27, 6)	(505, 53)	)	0.6249594797343507	0.9512195121951219	0
(40, 513, 27, 1)	(513, 53)	|	1.0	1.0	0
(79, 525, 13, 9)	(529, 86)	k	0.6414472515079733	0.9344878217919581	0
(33, 524, 38, 36)	(539, 52)	\sum	0.8411653053740242	0.9872639880016522	4
(12, 535, 13, 12)	(541, 18)	\lambda	0.6368609677265646	0.7204239424448182	4
(85, 536, 5, 13)	(542, 87)	=	0.8319276568320804	0.9648635815536847	0
(12, 546, 5, 4)	(547, 13)	\text{r}	0.6233790733514061	0.8245883961385941	0
(79, 551, 13, 8)	(555, 85)	0	0.6662763727108042	0.9568267108223655	0
(49, 568, 11, 6)	(570, 54)	\epsilon	0.6471086299745521	0.8143046618229481	0
(48, 573, 5, 5)	(575, 49)	\rightharpoondown	0.6191103697605549	0.7343467858190724	3
(58, 575, 1, 1)	(575, 58)	\blacksquare	0.927639548250941	0.9738108599560538	3
(57, 577, 1, 1)	(577, 57)	\blacksquare	0.8887201389344801	0.9738108599560538	3
(43, 581, 1, 12)	(586, 43)	-	0.8027651037744293	0.9600319616511285	0
(40, 595, 8, 10)	(599, 44)	\alpha	0.557325814706936	0.8659196953692019	0
(41, 605, 1, 1)	(605, 41)	\blacksquare	0.9267089330849527	0.9738108599560538	0
(35, 608, 13, 9)	(611, 42)	k	0.6667536901956297	0.9171329209534959	0
(22, 624, 61, 25)	(637, 52)	\int	0.8236222718957803	0.7543316689271135	5
(73, 639, 11, 5)	(641, 78)	t	0.6599091143311133	0.9012270403350411	5
(79, 647, 1, 12)	(652, 79)	-	0.8007422116349886	0.9600319616511285	3
(18, 651, 11, 6)	(653, 23)	t	0.7364316773540476	0.9506135201675205	3
(24, 659, 1, 12)	(664, 24)	-	0.8007422116349886	0.9600319616511285	3
(71, 662, 13, 8)	(665, 78)	k	0.6480698415704764	0.9344878217919581	3
(16, 674, 13, 4)	(676, 22)	l	0.5646925925594357	0.8589698515833195	1
(79, 673, 1, 12)	(678, 79)	-	0.8027651037744293	0.9600319616511285	0
(25, 678, 4, 4)	(679, 27)	\lfloor	0.4984705874153188	0.8104350558471942	2
(21, 680, 3, 3)	(681, 22)	\text{l}	0.5432348103038203	0.8639959198163908	2
(71, 688, 13, 6)	(690, 78)	1	0.7788550466860941	0.9332591355734	0
(41, 703, 19, 19)	(710, 49)	C	0.7785789898641748	0.9512340150905829	0
(40, 726, 27, 6)	(727, 53)	(	0.614451802574221	0.9512195121951219	0
(48, 735, 12, 10)	(740, 53)	s	0.6546003878374803	0.9586903807613987	0
(40, 748, 27, 6)	(751, 53)	)	0.761176477074688	0.975609756097561	0
(41, 762, 19, 13)	(769, 52)	d	0.7235141696994037	0.9592091491775998	1
(48, 776, 12, 11)	(782, 54)	s	0.6855544392543803	0.9586903807613987	1

Case05-L2-H
Time: 0.5783271789550781

Position (y, x, h, w)	Centroid (x, y)	Answer	Similarity	2nd Similarity	Depth
(94, 4, 72, 34)	(24, 135)	j	0.8439512790537298	0.9508823327587399	0
(94, 46, 56, 23)	(58, 126)	i	0.794103211752953	0.9524348505845506	0
(94, 75, 56, 23)	(87, 126)	i	0.794103211752953	0.9524348505845506	0
(94, 103, 56, 23)	(115, 126)	i	0.794103211752953	0.9524348505845506	0
(124, 155, 9, 9)	(159, 128)	\cdot	0.675605899586397	0.8232233047033631	0
(2, 219, 51, 26)	(234, 32)	j	0.8432893949510093	0.9450847785761639	6
(208, 226, 40, 18)	(235, 231)	i	0.8264860018239998	0.9663663603001844	6
(70, 194, 117, 111)	(242, 130)	\sum	0.9026867636132095	0.9872639880016522	6
(208, 246, 51, 26)	(261, 238)	j	0.8432893949510093	0.9644777583337306	6
(2, 250, 51, 26)	(265, 32)	j	0.8432893949510093	0.9450847785761639	6
(94, 323, 72, 34)	(343, 135)	j	0.8439512790537298	0.9508823327587399	1
(124, 388, 9, 9)	(392, 128)	\cdot	0.675605899586397	0.8232233047033631	1
(70, 426, 117, 111)	(474, 130)	\sum	0.9026867636132095	0.9872639880016522	4
(6, 474, 40, 18)	(483, 29)	i	0.8264860018239998	0.9538979554442426	4

L2 Pixelwise Similarity + Chamfer recheck

Similarity Threshold = 0.7; Second Similarity Threshold = 0.985

Figure 22: Case 01, L2 + Chamfer

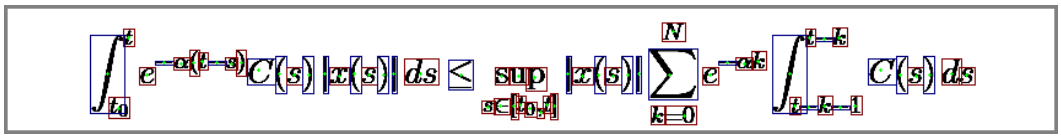

Figure 23: Case 02, L2 + Chamfer

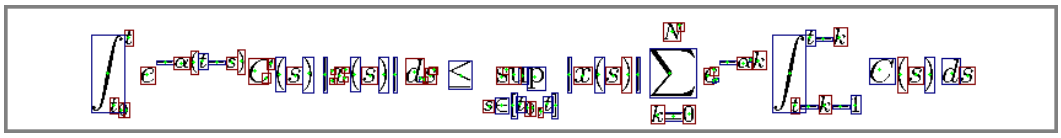

Figure 24: Case 03, L2 + Chamfer

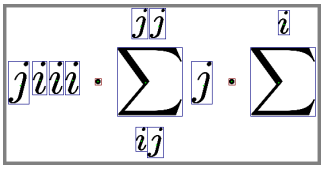

Figure 25: Case 05, L2 + Chamfer

```
Case01-L2-C
Time: 0.05372452735900879
+-----------------------+-----------------+--------+--------------------+--------------------+-------+
| Position (y, x, h, w) | Centroid (x, y) | Answer |     Similarity     |   2nd Similarity   | Depth |
+-----------------------+-----------------+--------+--------------------+--------------------+-------+
|     (12, 2, 12, 7)    |     (5, 18)     |   t    | 0.6501996994903936 | 0.9923610632462397 |   0   |
+-----------------------+-----------------+--------+--------------------+--------------------+-------+

Case02-L2-C
Time: 1.8138980865478516
+-----------------------+-----------------+----------------+--------------------+--------------------+-------+
| Position (y, x, h, w) | Centroid (x, y) |     Answer     |     Similarity     |   2nd Similarity   | Depth |
+-----------------------+-----------------+----------------+--------------------+--------------------+-------+
|    (22, 68, 61, 26)   |     (81, 52)    |      \int      | 0.8112695466053161 | 0.9843964497850461 |   0   |
|    (72, 83, 15, 15)   |     (90, 80)    |    \text{k}    | 0.48111248463144873 | 0.9687120441472112 |   0   |
|    (17, 95, 12, 7)    |     (98, 23)    |       t        | 0.6412090482077021 | 0.9921126269600911 |   0   |
|   (48, 108, 12, 11)   |    (113, 53)    |       c        | 0.6302641111334014 | 0.9872485570537994 |   0   |
|    (43, 121, 1, 13)   |    (127, 43)    |       -        | 0.8007422116349886 | 0.9992313838779063 |   0   |
|    (40, 136, 8, 12)   |    (141, 44)    |     \alpha     | 0.5636751742760288 | 0.9910398216021798 |   0   |
|    (34, 149, 19, 6)   |    (151, 43)    |       (        | 0.6800281140816784 | 0.9948141402412572 |   1   |
|    (36, 156, 12, 6)   |    (158, 42)    |       t        | 0.5509637992098394 | 0.9896422086331647 |   1   |
|    (43, 164, 1, 13)   |    (170, 43)    |       -        | 0.8007422116349886 | 0.9992313838779063 |   0   |
|    (40, 178, 8, 8)    |    (182, 44)    |     \cdot      | 0.5336386048560049 | 0.9484401305384809 |   0   |
|    (34, 187, 19, 6)   |    (190, 43)    |       )        | 0.6984232397013816 | 0.9959876646805674 |   0   |
|   (41, 196, 19, 21)   |    (204, 49)    |       C        | 0.7489220313776552 | 0.995805424297517  |   0   |
|    (39, 219, 28, 7)   |    (221, 52)    |       (        | 0.7395491111297813 | 0.9967567599842723 |   0   |
|   (48, 228, 12, 11)   |    (233, 53)    |       s        | 0.6442742711748131 | 0.9933883954603301 |   0   |
|    (39, 241, 28, 7)   |    (245, 53)    |       )        | 0.7257545814123264 | 0.9965447154471545 |   0   |
|    (39, 258, 28, 2)   |    (258, 52)    |       \|       |        1.0         |        1.0         |   0   |
|   (48, 263, 12, 14)   |    (270, 54)    |       x        | 0.616991876571773  | 0.9928938404667408 |   0   |
|    (39, 280, 28, 7)   |    (282, 52)    |       (        | 0.7395491111297813 | 0.9967567599842723 |   0   |
```

(48, 289, 12, 11)	(294, 53)	s	0.6442742711748131	0.9933883954603301	0
(39, 302, 28, 7)	(306, 53)	)	0.7208980172688736	0.9957599028410242	0
(39, 314, 28, 2)	(314, 52)	|	0.972294003887706	1.0	0
(41, 324, 19, 26)	(336, 52)	L	0.5090748163863589	0.9654938083321855	0
(42, 360, 22, 18)	(369, 53)	\leq	0.785439400295016	0.9959994064275194	0
(75, 387, 8, 9)	(391, 79)	s	0.5725621765910893	0.9900540300436511	0
(73, 397, 11, 11)	(401, 78)	\in	0.6917619024564499	0.9934666966190748	3
(48, 398, 12, 10)	(402, 54)	\text{s}	0.6458485552135702	0.9937478041110738	3
(69, 411, 19, 4)	(412, 78)	[	0.6489462442853158	0.9964292571306377	5
(48, 409, 12, 14)	(416, 54)	\text{n}	0.627418862649586	0.9919481456720667	4
(71, 415, 12, 6)	(417, 77)	t	0.5509637992098394	0.9896422086331647	5
(76, 422, 10, 8)	(425, 80)	0	0.55120206820204	0.9900524245194917	0
(48, 423, 17, 15)	(429, 55)	\text{p}	0.6809162258061873	0.9944387979631886	0
(81, 432, 6, 4)	(434, 83)	,	0.5989129648050695	0.9841207325438895	0
(71, 437, 12, 6)	(439, 77)	t	0.5509637992098394	0.9896422086331647	0
(69, 443, 19, 4)	(445, 78)	]	0.6462592496082983	0.9963140330916971	0
(39, 456, 28, 2)	(456, 52)	|	0.972294003887706	1.0	0
(48, 461, 12, 15)	(468, 54)	x	0.630689683546971	0.9914043311641592	0
(39, 479, 28, 7)	(481, 53)	(	0.7126966312204062	0.9957811825840156	0
(48, 487, 12, 12)	(493, 54)	s	0.6599998354065117	0.9933296085389572	0
(39, 501, 28, 7)	(505, 53)	)	0.7120520177480982	0.9957317073170732	0
(39, 513, 28, 2)	(514, 52)	|	1.0	1.0	0
(79, 525, 13, 10)	(529, 86)	k	0.5758825872966433	0.9914993350993432	0
(33, 523, 39, 38)	(539, 53)	\sum	0.8047063556258368	0.998658112181978	4
(12, 534, 13, 17)	(542, 18)	N	0.6546182481105398	0.9946213637233691	4
(79, 536, 13, 24)	(551, 86)	\longrightarrow	0.5455451124910109	0.9737809370463364	0
(48, 567, 12, 11)	(572, 53)	c	0.6359622330989851	0.9884579140673504	0
(43, 580, 1, 13)	(586, 43)	-	0.8007422116349886	0.9992313838779063	0
(40, 594, 8, 12)	(600, 44)	\alpha	0.5101686826599887	0.9886884936849081	0
(35, 607, 13, 10)	(611, 42)	k	0.5457637879691819	0.9889372487970257	0
(22, 624, 61, 26)	(637, 52)	\int	0.8481457206272577	0.9885723120281471	5
(72, 638, 12, 7)	(641, 78)	t	0.5944584485237567	0.9892324905733441	5
(79, 646, 1, 13)	(652, 79)	-	0.8007422116349886	0.9992313838779063	3
(17, 651, 12, 6)	(653, 23)	t	0.5509637992098394	0.9896422086331647	3
(24, 659, 1, 13)	(665, 24)	-	0.8007422116349886	0.9992313838779063	3
(71, 661, 13, 10)	(665, 78)	k	0.5730413840756658	0.9912248189224879	3
(16, 673, 13, 10)	(677, 23)	k	0.5457637879691819	0.9889372487970257	3
(79, 672, 1, 13)	(678, 79)	-	0.8007422116349886	0.9992313838779063	3
(71, 688, 13, 7)	(690, 78)	\text{l}	0.662755472202137	0.992034456654834	0
(41, 702, 19, 21)	(711, 49)	C	0.7515082146139705	0.9956743529854594	0
(39, 725, 28, 7)	(727, 53)	(	0.7397297097623259	0.9966659058301813	1
(48, 734, 12, 11)	(740, 54)	s	0.6045913594976304	0.9910415333317126	1
(39, 747, 28, 7)	(751, 53)	)	0.7208980172688736	0.9957599028410242	1
(41, 762, 19, 14)	(769, 52)	d	0.5913285615589079	0.9905639624998505	1
(48, 776, 12, 11)	(781, 53)	s	0.6442742711748131	0.9933883954603301	1

Case03-L2-C
Time: 2.5458130836486816

Position (y, x, h, w)	Centroid (x, y)	Answer	Similarity	2nd Similarity	Depth
(22, 69, 61, 25)	(81, 52)	\int	0.8804873393286075	0.9883786243395991	0
(73, 84, 11, 5)	(86, 78)	t	0.6441517116959318	0.9908967547796858	0
(77, 91, 10, 3)	(92, 82)	(	0.6512793367097558	0.9925631954742102	0
(77, 95, 10, 3)	(96, 82)	\}	0.5426730137681869	0.9876695161549114	0
(18, 96, 11, 5)	(98, 23)	t	0.6471690877559237	0.9927942493233284	0
(48, 109, 12, 10)	(113, 53)	e	0.6560078584840772	0.9897676440159678	0
(43, 122, 1, 12)	(128, 43)	-	0.8007422116349886	0.9992313838779063	0
(40, 136, 8, 11)	(141, 44)	\alpha	0.6401934020661277	0.99303619593157	0
(35, 150, 17, 4)	(151, 43)	(	0.6625122926824529	0.9937868042911754	1
(37, 156, 11, 6)	(158, 42)	t	0.7364316773540476	0.9957962301081443	1
(43, 164, 1, 12)	(170, 43)	-	0.8007422116349886	0.9992313838779063	0
(40, 179, 8, 7)	(182, 43)	S	0.5909722944389066	0.9899047818161499	0
(34, 188, 18, 4)	(190, 42)	)	0.6608101168813563	0.9937227886975715	0
(41, 197, 19, 14)	(201, 50)	\mathcal{C}	0.6502051924982701	0.9836585774331054	0
(53, 208, 6, 5)	(210, 56)	/	0.655018894273272	0.9844607344397801	2
(41, 212, 7, 4)	(214, 44)	\bigstar	0.4852629735258074	0.9666358951725142	2
(40, 219, 26, 6)	(221, 53)	(	0.7892597890311289	0.9967825635703166	1
(48, 228, 12, 11)	(234, 54)	s	0.6855544392543803	0.9922013616016846	0
(40, 241, 27, 7)	(245, 52)	)	0.7495430077581059	0.995364921764024	0
(40, 258, 27, 1)	(258, 53)	|	1.0	1.0	0
(50, 264, 2, 2)	(264, 50)	l	0.5325919575934173	0.9815581988890082	3
(57, 263, 3, 4)	(264, 58)	\cdot	0.574616268382353	0.9803581449670403	3
(48, 267, 12, 6)	(270, 54)	\text{l}	0.5866503869395692	0.9873673014222473	0
(56, 274, 2, 2)	(274, 56)	l	0.5333415253571769	0.981686520054095	3
(48, 273, 3, 4)	(275, 49)	,	0.5552620223174003	0.9789254397112755	3
(40, 280, 26, 6)	(282, 53)	(	0.7892597890311289	0.9967825635703166	0
(48, 289, 12, 11)	(295, 54)	s	0.6855544392543803	0.9922013616016846	0
(40, 303, 27, 6)	(306, 53)	)	0.761176477074688	0.9959525569281666	0
(40, 315, 27, 1)	(315, 53)	|	1.0	1.0	0
(41, 325, 19, 13)	(331, 51)	d	0.6252310555453302	0.9899744201348628	1
(56, 336, 2, 1)	(336, 56)	\blacksquare	0.9267089330849527	0.9999832977423189	2
(56, 339, 3, 2)	(339, 57)	\blacksquare	0.6373230835302871	0.9902589804401682	2
(49, 341, 11, 7)	(344, 54)	\text{S}	0.5349218701977737	0.9833875848535063	2
(48, 344, 4, 5)	(347, 49)	\daleth	0.5445688167622816	0.9803066246167775	2
(43, 360, 21, 17)	(369, 54)	\leq	0.7330452125125746	0.9954949139867582	0
(75, 388, 8, 7)	(392, 79)	\mathcal{S}	0.5956813076357885	0.9892400039356637	0
(48, 399, 12, 8)	(402, 55)	\text{S}	0.640798997041333	0.9920420366630727	0
(73, 398, 11, 9)	(402, 78)	\in	0.7280378688993686	0.9940084501155451	0
(48, 404, 4, 3)	(406, 49)	]	0.5875483375106125	0.987870689488328	0
(69, 411, 19, 3)	(411, 78)	[	0.8584386780943228	0.9995252769595645	4
(48, 409, 12, 8)	(412, 53)	\text{t}	0.622810586340846	0.9744280941035285	4
(72, 415, 11, 6)	(417, 77)	t	0.7364316773540476	0.9957962301081443	3
(48, 417, 12, 6)	(419, 54)	\text{l}	0.7602832897434025	0.9966527637385253	3
(76, 422, 10, 3)	(423, 80)	(	0.5447595728141809	0.9906642393915147	0
(76, 426, 10, 3)	(427, 80)	)	0.6522993797258271	0.9936674013954355	3
(48, 424, 17, 13)	(429, 55)	\text{p}	0.7034994173092948	0.9930845840591124	3
(81, 433, 6, 2)	(434, 83)	,	0.553059929809641	0.9831458730919341	0
(72, 437, 11, 6)	(439, 77)	t	0.7364316773540476	0.9957962301081443	0
(69, 444, 19, 3)	(446, 78)	]	0.8557352334757056	0.9994100529206239	0
(40, 457, 27, 1)	(457, 53)	|	1.0	1.0	0

(48, 462, 12, 13)	(468, 54)	x	0.6789572519240435	0.9922149011216916	0
(40, 479, 27, 6)	(481, 53)	(	0.7669114943388973	0.9956595281964926	0
(48, 488, 12, 10)	(493, 54)	s	0.6567378325176901	0.990941431282502	0
(40, 501, 27, 6)	(505, 53)	)	0.6249594797343507	0.9903943980498564	0
(40, 513, 27, 1)	(513, 53)	|	1.0	1.0	0
(79, 525, 13, 9)	(529, 86)	k	0.6414472515079733	0.9906948865260685	0
(33, 524, 38, 36)	(539, 52)	\sum	0.8411653053740242	0.9990485637547387	4
(12, 535, 13, 12)	(541, 18)	\lambda	0.6368609677265646	0.9751700780464935	4
(85, 536, 5, 13)	(542, 87)	=	0.8319276568320804	0.9993725639563158	0
(12, 546, 5, 4)	(547, 13)	\text{r}	0.6233790733514061	0.9865490680356449	0
(79, 551, 13, 8)	(555, 85)	0	0.6662763727108042	0.9959163513438614	0
(49, 568, 11, 6)	(570, 54)	\epsilon	0.6471086299745521	0.9872017814966199	0
(48, 573, 5, 5)	(575, 49)	\rightharpoondown	0.6191103697605549	0.9707176045101464	3
(58, 575, 1, 1)	(575, 58)	\blacksquare	0.927639548250941	0.9999832977423189	3
(57, 577, 1, 1)	(577, 57)	\blacksquare	0.8887201389344801	0.9999832977423189	3
(43, 581, 1, 12)	(586, 43)	-	0.8027651037744293	0.9992313838779063	0
(40, 595, 8, 10)	(599, 44)	\alpha	0.557325814706936	0.9867632079330648	0
(41, 605, 1, 1)	(605, 41)	\blacksquare	0.9267089330849527	0.9999832977423189	0
(35, 608, 13, 9)	(611, 42)	k	0.6667536901956297	0.990344093222219	0
(22, 624, 61, 25)	(637, 52)	\int	0.8236222718957803	0.9902707355440981	5
(73, 639, 11, 5)	(641, 78)	t	0.6599091143311133	0.9912331975986025	5
(79, 647, 1, 12)	(652, 79)	-	0.8007422116349886	0.9992313838779063	3
(18, 651, 11, 6)	(653, 23)	t	0.7364316773540476	0.9957962301081443	3
(24, 659, 1, 12)	(664, 24)	-	0.8007422116349886	0.9992313838779063	3
(71, 662, 13, 8)	(665, 78)	k	0.6480698415704764	0.9912058683379049	3
(16, 674, 13, 9)	(677, 23)	k	0.6667536901956297	0.9905569125545978	0
(79, 673, 1, 12)	(678, 79)	-	0.8027651037744293	0.9992313838779063	0
(71, 688, 13, 6)	(690, 78)	1	0.7788550466860941	0.996662620238981	0
(41, 703, 19, 19)	(710, 49)	C	0.7785789898641748	0.9958234213695515	0
(40, 726, 27, 6)	(727, 53)	(	0.614451802574221	0.9892720520776794	0
(48, 735, 12, 10)	(740, 53)	s	0.6546003878374803	0.9919630630220068	0
(40, 748, 27, 6)	(751, 53)	)	0.761176477074688	0.9959525569281666	0
(41, 762, 19, 13)	(769, 52)	d	0.7235141696994037	0.9947517843313528	1
(48, 776, 12, 11)	(782, 54)	s	0.6855544392543803	0.9922013616016846	1

Case05-L2-C
Time: 0.5791270732879639

Position (y, x, h, w)	Centroid (x, y)	Answer	Similarity	2nd Similarity	Depth
(94, 4, 72, 34)	(24, 135)	j	0.8439512790537298	0.99551625275265	0
(94, 46, 56, 23)	(58, 126)	i	0.794103211752953	0.9963112358651984	0
(94, 75, 56, 23)	(87, 126)	i	0.794103211752953	0.9963112358651984	0
(94, 103, 56, 23)	(115, 126)	i	0.794103211752953	0.9963112358651984	0
(124, 155, 9, 9)	(159, 128)	\cdot	0.675605899586397	0.9873730931930974	0
(2, 219, 51, 26)	(234, 32)	j	0.8432893949510093	0.9935345547958635	6
(208, 226, 40, 18)	(235, 231)	i	0.8264860018239998	0.9974068196341481	6
(70, 194, 117, 111)	(242, 130)	\sum	0.9026867636132095	0.9995812486844352	6
(208, 246, 51, 26)	(261, 238)	j	0.8432893949510093	0.9971845797330895	6
(2, 250, 51, 26)	(265, 32)	j	0.8432893949510093	0.9940586988316582	6
(94, 323, 72, 34)	(343, 135)	j	0.8439512790537298	0.99551625275265	1
(124, 388, 9, 9)	(392, 128)	\cdot	0.675605899586397	0.9873730931930974	1
(70, 426, 117, 111)	(474, 130)	\sum	0.9026867636132095	0.9995812486844352	4
(6, 474, 40, 18)	(483, 29)	i	0.8264860018239998	0.9936281130702643	4

Some Results from Case 04

The following pictures show some extra results from Case 04.

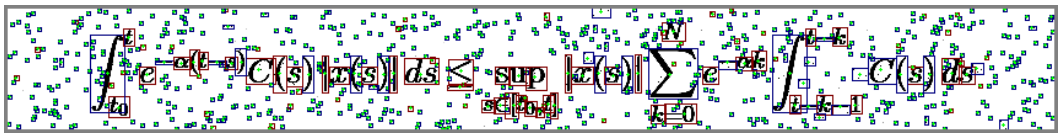

Figure 26: A clustering result for Case 04 using L2 Pixelwise Similarity

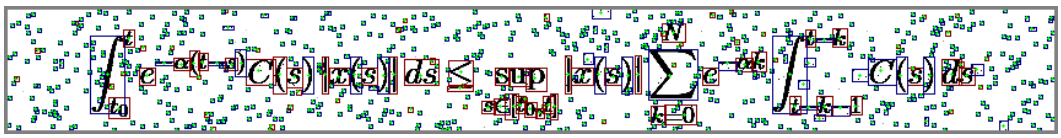

Figure 27: A clustering result for Case 04 using Chamfer Similarity

Template Library of Mathematical Symbols

This section provides a comprehensive overview of the template library, which comprises all 459 mathematical symbols utilized in this study.

```
0 1 2 3 4 5 6 7 8 9
a b c d e f g h i j k l m n o p q r s t u v w x y z
A B C D E F G H I J K L M N O P Q R S T U V W X Y Z
\text{a} \text{b} \text{c} \text{d} \text{e} \text{f} \text{g} \text{h} \text{i} \text{j}
\text{k} \text{l} \text{m} \text{n} \text{o} \text{p} \text{q} \text{r} \text{s} \text{t}
\text{u} \text{v} \text{w} \text{x} \text{y} \text{z}
\text{A} \text{B} \text{C} \text{D} \text{E} \text{F} \text{G} \text{H} \text{I} \text{J}
\text{K} \text{L} \text{M} \text{N} \text{O} \text{P} \text{Q} \text{R} \text{S} \text{T}
\text{U} \text{V} \text{W} \text{X} \text{Y} \text{Z}
+ - * / | \| ( ) = [ ] \{ \} , \lfloor \rfloor \lceil \rceil
\alpha \beta \gamma \delta \epsilon \varepsilon \zeta \eta \theta \vartheta \iota
\kappa \lambda \mu \nu \xi \pi \varpi \rho \varrho
\sigma \varsigma \tau \upsilon \phi \varphi \chi \psi \omega
\Gamma \varGamma \Delta \varDelta \Theta \varTheta \Lambda \varLambda \Xi \varXi \Pi \varPi
\Sigma \varSigma \Upsilon \varUpsilon \Phi \varPhi \Psi \varPsi \Omega \varOmega
\aleph \beth \daleth \gimel
\sum \prod \coprod \int \oint \iint \bigcap \bigcup \bigoplus \bigotimes \bigodot \bigsqcup
\ast \star \cdot \circ \diamond \times \div \circledast \circledcirc
\circleddash \pm \mp \amalg \odot \oplus \otimes \Box \boxplus \cap \cup
\sqcap \sqcup \wedge \vee \dagger \ddagger \intercal \lhd \rhd
\unlhd \unrhd \bigtriangledown \bigtriangleup \equiv \cong \neq \sim \simeq \approx
\propto \models \leq \geq \prec \succ \preceq \succeq \ll \gg \subset \supset \subseteq \supseteq
\perp \parallel \in \ni \notin \triangleq \doteqdot \thickapprox \fallingdotseq \risingdotseq
\therefore \because \leqq \geqq \leqslant \geqslant \lessapprox \gtrapprox \subseteqq \supseteqq
\preccurlyeq \succcurlyeq \Vdash \ncong \nparallel \ntriangleleft \ntrianglelefteq \ntriangleright
\ntrianglerighteq \nleq \ngeq \nleqq \ngeqq \nleqslant \ngeqslant \nless \ngtr \nprec \nsucc \npreceq \nsucceq
\lneq \gneq \lneqq \gneqq \nsubseteq \nsupseteq \nsubseteqq \nsupseteqq \subsetneq \supsetneq
\subsetneqq \supsetneqq \leftarrow \longleftarrow \Leftarrow \Longleftarrow \rightarrow \longrightarrow
\Rightarrow \Longrightarrow \leftrightarrow \longleftrightarrow \Leftrightarrow \Longleftrightarrow
\uparrow \Uparrow \downarrow \Downarrow \updownarrow \Updownarrow \nleftarrow \nrightarrow
\nLeftarrow \nRightarrow \nleftrightarrow \nLeftrightarrow \mapsto \longmapsto
\hookleftarrow \hookrightarrow \leftharpoonup \rightharpoonup \leftharpoondown \rightharpoondown
\rightleftharpoons \leftrightharpoons \upharpoonleft \downharpoonleft \upharpoonright \downharpoonright
\nearrow \searrow \swarrow \nwarrow \leftleftarrows \rightrightarrows \leftrightarrows \rightleftarrows
\upuparrows \downdownarrows \curvearrowleft \curvearrowright
\infty \nabla \partial \eth \clubsuit \diamondsuit \heartsuit \spadesuit
\Im \Re \forall \exists \nexists \emptyset \varnothing \ell \bigstar \hbar \hslash \mho
\wp \angle \measuredangle \sphericalangle \complement \blacksquare
\mathcal{A} \mathcal{B} \mathcal{C} \mathcal{D} \mathcal{E} \mathcal{F} \mathcal{G} \mathcal{H}
\mathcal{I} \mathcal{J} \mathcal{K} \mathcal{L} \mathcal{M} \mathcal{N} \mathcal{O} \mathcal{P}
\mathcal{Q} \mathcal{R} \mathcal{S} \mathcal{T} \mathcal{U} \mathcal{V} \mathcal{W} \mathcal{X}
\mathcal{Y} \mathcal{Z}
\mathbb{A} \mathbb{B} \mathbb{C} \mathbb{D} \mathbb{E} \mathbb{F} \mathbb{G} \mathbb{H}
\mathbb{I} \mathbb{J} \mathbb{K} \mathbb{L} \mathbb{M} \mathbb{N} \mathbb{O} \mathbb{P}
\mathbb{Q} \mathbb{R} \mathbb{S} \mathbb{T} \mathbb{U} \mathbb{V} \mathbb{W} \mathbb{X}
\mathbb{Y} \mathbb{Z}
\mathfrak{A} \mathfrak{B} \mathfrak{C} \mathfrak{D} \mathfrak{E} \mathfrak{F} \mathfrak{G}
\mathfrak{H} \mathfrak{I} \mathfrak{J} \mathfrak{K} \mathfrak{L} \mathfrak{M} \mathfrak{N}
\mathfrak{O} \mathfrak{P} \mathfrak{Q} \mathfrak{R} \mathfrak{S} \mathfrak{T} \mathfrak{U}
\mathfrak{V} \mathfrak{W} \mathfrak{X} \mathfrak{Y} \mathfrak{Z}
```